
UNIVERSITY OF BIRMINGHAM

# Targeted Assessment of the Glycolytic Enzyme Content of Extracellular Vesicles in the Context of Exercise

**Student ID:** [redacted]

**Supervisor: Dr Martin Whitham**

**Word Count: 15328**

**School of Sport, Exercise and Rehabilitation Sciences**

# ABSTRACT

Exercise, capable of greatly increasing intracellular glycolytic rate, has frequently been shown to also induce an increase in circulating exosome-like-vesicles (ELVs) (Frühbeis et al, 2015; Whitham et al, 2018; Brahmer et al, 2019). However, the physiological relevance of ELVs in this context remains elusive. Attempts to unravel the cargo proteome, and therefore potential function, of exercise-mediated ELVs have unexpectedly revealed the expression, and dynamic regulation via exercise, of multiple glycolytic enzymes (Whitham et al, 2018; Vanderboom et al, 2021). Though, some data has contradicted this finding (Jeppesen et al, 2019), and the physiological function of such ELVs enriched with glycolytic enzymes remains unclear. The aim of the present study was therefore to confirm the presence of glycolytic enzymes in ELVs isolated from both murine C2C12 myotube conditioned media and human plasma and test the hypothesis that their expression is modulated by glucose availability and high intensity exercise.

Western blots confirmed the presence of multiple glycolytic enzymes alongside classic ELV markers ALIX, TSG101, Syntenin 1 and CD9 in ELV lysates from conditioned media of C2C12 myotubes following both ultracentrifugation (UC) and size exclusion chromatography (SEC) isolation. Furthermore, culturing C2C12 myotubes in high glucose (HG) versus low glucose (LG) media, to assess the role of glucose availability on ELV glycolytic enzyme content, induced a significant ($p<0.05$) reduction in the expression of GAPDH, PGK1, PMK1, PKM2 and PD in ELVs isolated via UC. Subsequently, in human tetraspanin-positive ELV samples in vivo, we observed the presence of GAPDH at single EV resolution microarray level and dynamic regulation of glycolytic enzymes in response to an exhaustive bout of exercise following immunomagnetic isolation.

These data overall demonstrate that glycolytic enzymes are detected in murine muscle cell-derived ELVs in vitro, irrespective of isolation method and are responsive to glucose availability. Furthermore, glycolytic enzymes GAPDH and HKII are present in tetraspanin-positive ELVs in human plasma and are increased in circulation with exercise; supporting the proposition that ELVs transport glycolytic enzymes during the metabolic stress of exercise.

## ACKNOWLEDGEMENTS

I would primarily like to acknowledge and express my gratitude to Dr Martin Whitham for his continued academic guidance throughout the project, along with his willingness to go above and beyond to support my progress in the face of many barriers relating to the COVID-19 pandemic.

I would also like to acknowledge Dr Alex Seabright for aiding and supporting me in all experimental aspects of the study. I would specifically like to thank Sam Weaver, Hannah-Jade Parker, and Dr Sam Lucas for aiding in the exercise protocol and blood collection and handling. I would finally like to thank Dr Luke McIlvenna for aiding with the ExoView™ analysis, the only experimental aspect not completed by myself.

# TABLE OF CONTENTS

# 1. INTRODUCTION

## 1.1 Introduction:

The finding that exercise, in multiple forms, induces a release of extracellular vesicles (EVs) into the circulation is intriguing (Frühbeis et al, 2015; Whitham et al, 2018; Brahmer et al, 2019), and has prompted much discussion in the literature. Extracellular vesicles are defined as heterogenous, membranous nano-sized vesicles released from the majority of cells and are believed to have potent autocrine and paracrine functions (Maas et al, 2017). Though early suggestions have been made, the physiological relevance behind this exercise-mediated EV release remains largely unclear. It is widely accepted that EVs are able to communicate between cells and tissues via the horizontal transfer of their biologically active cargo (Whitham et al, 2018), and therefore analysis of their cargo proteome may allude somewhat to their function. Proteome enrichment analyses of exercise-mediated EVs (Whitham et al, 2018; Vanderboom et al, 2021) have unexpectedly demonstrated an overrepresentation of proteins involved in key metabolic processes following exercise. Therefore, it could be hypothesised that EVs and their respective cargo proteome may play a role in aiding the multi-tissue metabolic response via the transfer of metabolically active proteins between cells and tissues.

## 1.2 An Introduction to EVs:

Intercellular communication via circulating proteins in the context of exercise was first hypothesized over 60 years ago (Goldstein, 1961; Kao & Ray, 1954), and has since been described in a multitude of tissues (Febbraio et al, 2004; Moon et al, 2016; Rao et al, 2014; Hansen et al, 2011; Hondares et al, 2011; Lancaster et al, 2014) via proteins termed myokines

(Pedersen et al, 2003). There have been many suggestions that the exercise-induced secretome may have a role in mediating the physiological responses and adaptations to exercise. A prominent example, in the context of the present study, is IL-15 (interleukin-15); described to alter glucose metabolism in the target cell during exercise by regulating cellular glucose uptake and consequent metabolic homeostasis (Busquets et al, 2006; Barra et al, 2012). However, in the context of myokines, the relative amount of such proteins that are released during exercise is relatively small compared to the abundance already residing in cells. This has led to the questioning of how such a small amount of one singular secreted protein (such as IL-15) can possibly be mediating such large and complex physiological effects in vivo in response to exercise, particularly given the frequent need for a receptor on the target cell that not all cells can possess. Therefore, in more recent years there has been a shift in focus towards a novel means of tissue crosstalk that attempts to overcome these claims; EV trafficking.

EVs are inconsistently sub grouped based on size, morphology or cellular origin, with the latter giving rise to "exosomes" originating from multi vesicular bodies (MVB) in the endocytic pathway, and microvesicles and apoptotic bodies thought to simply bleb off the plasma membrane. The endocytic pathway is a complex biogenesis pathway, first discovered in the 1980s (Pan et al, 1985; Harding et al, 1983), and is thought to separate exosomes' potential for physiological and pathological function from the other, arguably simpler, EV subtypes. Many of the proteins involved in exosome biogenesis via the endocytic pathway are implicated as putative exosome markers, such as CD9, CD63, CD81, ALIX, TSG101 and syntenin-1 (Kowal et al, 2016). While some markers may not be absolutely exclusive to exosomes, and therefore not exemplary (Kalra et al, 2012), they are a strong indication of the presence of exosomes in a sample. ALIX and syntenin-1 have been descried as some of the most abundantly detected markers in isolated exosome samples (Jeppesen et

al, 2019). More recently, syntenin-1 has been described as the most highly abundant putative universal exosome marker (Kugeratski et al, 2021). ALIX (ALG-2-interacting proteinX), part of the ESCRT-111 complex, is believed to interact with TSG101 (tumour susceptibility gene 101), part of the ESCRT-1 complex, to promote the budding of intraluminal vesicles (ILVs) into endosomes or a MVB (Baietti et al, 2012; Colombo et al, 2014). Silencing ALIX has previously led to decreased expression of exosomes (Colombo et al, 2014). The MVB is then translocated to the plasma membrane, where it is released into the extracellular space (Colombo et al, 2014). The size of the exosome is dictated by and equal to the size of the ILVs from which it originates (Raposo & Stoorvogel, 2013). The cooperative relationship has been investigated between ALIX, syntenin-1, and syndecan proteins and is believed to be vital in the biogenesis of exosomes (Baietti et al, 2012). Since syndecan-4 mRNA is recognised as being upregulated in muscle during exercise irrespective of variables such as age, training, status and muscle type (as shown by the Gene XX tool (Reibe et al, 2018)), it could be reasonable to suggest this pathway as a trigger of the exercise-mediated exosome release (Frühbeis et al, 2015; Whitham et al, 2018; Brahmer et al, 2019). It has also been described that ALIX may play a role in sorting the tetraspanins (namely CD9, CD63 and CD81) into the endosome (Larios et al, 2020). Tetraspanins CD9, CD63, and CD81 are thought to be widely present on the membrane of exosomes; enriched in late MVBs (Kowal et al, 2014), and may aid in further sorting exosome cargo but evidence is limited (Berditchevski and Odinstova, 2007).

Whilst it was originally thought that the ESCRT protein complex played the predominant role in exosome biogenesis (Raposo & Stoorvogel, 2013), it has more recently been implicated that Rab proteins may also play a vital role (Pegtel & Gould, 2019). Ostrowski et al (2010) described a role of Rab27a and Rab27b in MVB biogenesis and positioning, supported by data demonstrating a ~50-75% decrease in exosome release in vitro

with a short hairpin RNA knockdown of Rab27 proteins (Ostrowski et al, 2010), dependent on the cell line. A similar reduction in exosome release of ~50% was observed with an inhibition of Rab35 (Hsu et al, 2010). Furthermore, Rab11 has also been implicated in exosome biogenesis via the maturation of MVBs as induced by calcium (Savina et al, 2005). Since the majority of existing exosome research to date concerns immune and cancer cells, we are forced to make the assumption that exosomes from other sources, such as muscle cells, possess the same markers. More work is required in order to explore potential markers further, especially in muscle derived exosomes. However, since many of the discussed proteins are widely identified as putative universal exosome markers (Kugeratski et al, 2021) and are thought to be involved in exosome biogenesis, they provide useful means by which to potentially identify and isolate exosomes in a range of contexts.

By virtue of this complex biogenesis pathway, exosomes are believed to contain the most specifically packaged cargo of all the EV subtypes, a selective heterogenous pool of: proteins (derived from the endosomes, the postprandial membrane, and the cytosol) (Théry et al, 2001), lipids, and nucleic acids (mRNA and miRNA) (Valadi et al, 2007). The majority of proteins seen to reside in exosomes do not possess signal peptides, and therefore cannot conceivably exit a healthy cell in the absence of a vesicle. Further to transporting proteins out of the parent cell into the extracellular space and subsequently the circulation, it has been described that exosomes are able to transfer the cargo to a recipient cell (Montecalvo et al, 2012; Tian et al, 2013; Mulcahy et al, 2014; Garcia et al, 2016). Upon arrival at the target cell guided by surface proteins (Tkach and Théry, 2016), exosomes are thought to 'communicate' with the cells by one of three methods: inducing signalling via receptor-ligand interaction; being internalised by endocytosis/phagocytosis; by fusing with the target cell's membrane to deliver contents into the cytosol. Moreover, it has been shown that exosomes not only transport biologically active cargo, but also have the potential to act as independent,

metabolically active units capable of functional L-asparaginase activity in the microenvironment via Asrg11 (Iraci et al, 2017), and therefore potentially other metabolic functions. There have been many attempts to unravel the complex cargo of exosomes and therefore their potential function, as will be briefly discussed.

### 1.3 EV Isolation Methods:

In order to study exosomes, it is necessary to first isolate them from the chosen sample. However, a significant limitation in the EV field is the lack of a gold standard isolation method. Considerations and suggestions for exosome isolation are set out in the MISEV (minimal information for studies of extracellular vesicles) 2018 guidelines; a comprehensive attempt by the international EV society to provide consensus on appropriate methods and practises (Théry et al, 2018). In all methods there is an inevitable trade-off between specificity, relating to the purity of the sample and absence of contaminating non-EV molecules, and recovery, relating to the overall exosome yield compared to the total present in the original sample. Other factors may include cost and time effectiveness. The chosen isolation method should also depend on multiple factors including sample type, starting sample volume and downstream analysis. The most commonly used exosome isolation methods currently are ultracentrifugation (UC), size exclusion chromatography (SEC), density gradient (DG), and immunomagnetic isolation (IM); though new methods are continuously being sought. The relative specificity and recovery of these methods as described in the MISEV guidelines (Théry et al, 2018) are depicted in Figure 1, as adapted from Cocozza et al (2020). UC (used in conjuction with preliminary low speed centrifugation steps) and SEC are both ‘intermediate recovery, intermediate specificity’, whilst DG and IM are described as ‘high specificity’ low recovery’ methods (Théry et al, 2018). UC comprises

of spinning the sample at high speeds to pellet the exosome sample. UC is relatively time effective and known to produce a relatively high yield, yet may coelute subpopulations of other vesicle subtypes and lipoproteins known to fall within the same size and density ranges as exosomes (Brennan et al, 2019). A protocol consisting of two rounds of ultracentrifugation may yield a purer exosome sample, however a highly vigorous protocol may aggregate the exosome sample (Linares et al, 2015). The UC instrument is also very expensive and is therefore not available to all groups. Following UC, as with other less specific isolation methods, careful post isolation characterisation is necessary, as outlined in the MISEV 2018 guidelines (Théry et al, 2018). SEC isolation consists of feeding the sample through a commercially available column in order to fractionate it, whereby exosomes are thought to elute in earlier fractions with all other components eluting in later fractions. Since SEC also isolates exosomes based on size, it may also co-elute other types of vesicles and other contaminants such as lipoproteins that fall within the same size bracket (Brennan et al, 2019). DG comprises of stacking mediums of different densities to allow exosomes to settle at their equilibrium density relative to the medium. This method usually aims to isolate exosomes of densities between 1.11-1.19g/ml. However, it has been shown that different subtypes of EVs are present in this range (Kowal et al, 2014). More importantly, other substances such as platelets or lipoproteins are known to fall within this range (Linares et al, 2015). Any platelets remaining may release EVs of their own, thereby contaminating the sample (as seen in many studies, summarised in Vesiclepedia (Kalra et al, 2012)). IM isolation or immunoaffinity isolation aims to isolate exosomes via immobilising them based on specific markers. Though the specificity of this method is high, the selection of markers is of upmost importance as there is much controversy in the literature surrounding certain markers and whether or not they are specific to exosomes. In any event, the results will be biased towards EVs with the chosen markers, which may only be a small subpopulation. All isolation

methods will inevitably elute a unique population of vesicles and potentially contaminants, and it has therefore often been recommended to utilise multiple methods in conjunction (Brennan et al, 2020; Karimi et al, 2018; Muller et al, 2014; Nordin et al, 2015; Onódi et al, 2018).

Due to the lack of gold standard isolation method, and considering that it has proven near impossible to specifically define and isolate exosomes, they will henceforth be referred to as 'exosome-like-vesicles' (ELVs), to accommodate for the fact that ELV samples may not exclusively comprise of exosomes.

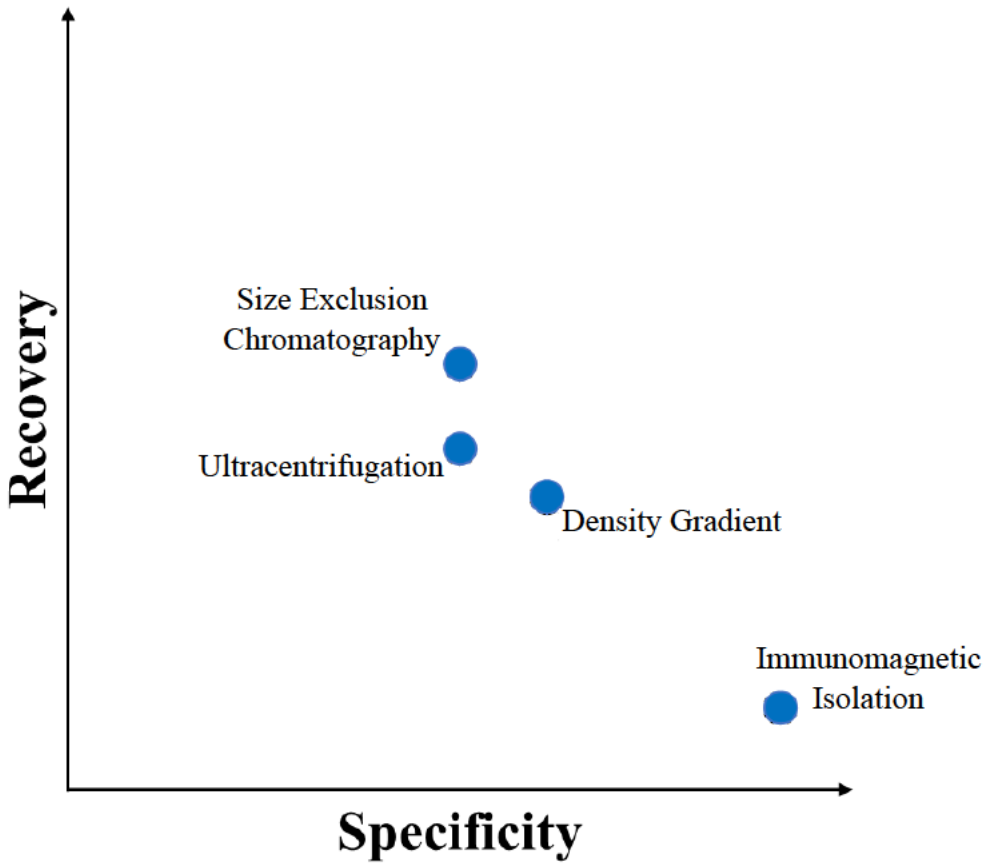


**Figure 1:** A graphical representation of the proposed specificity and recovery of the relevant exosome isolation methods, adapted from Cocozza et al, 2020.

## 1.4 ELVs and Exercise:

Conditions of physiological and metabolic stress, such as exercise, have been demonstrated as potential triggers for ELVs release into the circulation (Frühbeis et al, 2015; Whitham et al, 2018; Brahmer et al, 2019). An early study to hypothesise this, Frühbeis et al (2015), described via NTA (nanoparticle tracking analysis) and western blot analysis that following both incremental running and cycling exercise to exhaustion, vesicles with the size and marker profile of exosomes were increased in the circulation of healthy participants. However, as discussed, the use of size to categorise ELVs is outdated, as were many of the chosen ELV markers. Therefore, this data remains somewhat inconclusive. In 2019, it was shown that ELVs isolated from the plasma of healthy male athletes via SEC and IM isolation were increased in the circulation following an exhaustive incremental cycling test, via the detection (via western blot and flow cytometry) and increase of many markers including: CD9, C63, CD81, TSG101, and Syntenin-1 (Brahmer et al, 2019). A further, more in depth analysis revealed a transient increase in circulating ELVs following a 1-hour, exhaustive bout of cycling, with a rapid disappearance; insinuating an uptake into tissues (Whitham et al, 2018). Unbiased proteomic analysis of human plasma-derived ELV samples demonstrated an emergence of proteins known to constitute ELVs post exercise. Whitham and colleagues (2018) further demonstrated an uptake of ELVs into the murine liver using ELVs from donor mice labelled with lipophilic carbocyanine DiOC18 (7) (DiR) in C57BL6/J. Moreover, the ELVs isolated from exercised vs rest donors, when intravenously introduced into recipient mice showed greater uptake into the liver with equal dosing. The finding that exercise-mediated ELVs may demonstrate tropism to the liver may be significant in defining the extracellular response to exercise. In order to further understand this, analysis of the cargo of ELVs released as a result of exercise (believed to be specifically packaged (Zhao et al, 2016) and have the ability to alter the state of the target cell (Théry et al, 2001; Valadi et al, 2007;

Garcia et al, 2015)) may begin to unravel the physiological relevance of their release, which to date remains somewhat unclear. One possibility is that exercise-mediated ELVs may be aiding the metabolic response to exercise via the transfer of metabolically active cargo between cells and tissues.

## 1.5 An Introduction to Glycolysis:

Glycolysis, depicted in Figure 2, is a major metabolic pathway by which glucose is eventually converted to pyruvate and subsequently either acetyl coA or lactate, synthesising ATP molecules for energy (Gropper and Smith, 2012). From rest to exercise the demands for energy can increase by 100- fold, and failure to meet these demands is thought to cause much more rapid muscular fatigue (Sahlin et al, 1998). Alongside energy synthesis, glycolysis is also vital for the homeostatic control of blood insulin and glucose levels (Rossetti & Giacarri, 1990). The 10 core glycolytic enzymes each control a step in the glycolysis pathway: hexokinase (HK), phosphoglucose isomerase (PGI), phosphofructokinase (PFK), adolase (ALDOA), triose phosphate isomerase (TPI), glyceraldehyde-3-phosphate dehydrogenase (GAPDH), phosphoglycerate kinase (PGK), phosphoglyceratemutase (PGAM), enolase (ENO), and pyruvate kinase (PK) (Gropper & Smith, 2012). Details of each step are depicted in Figure 2. Lactate dehydrogenase (LDH), though not part of the central glycolytic chain, is fundamental in the conversion of pyruvate to lactate (considered an end product of glycolysis) in anaerobic conditions to synthesise NAD+; a vital component of the glycolytic chain (Farhana & Lappin, 2020). On the other hand, during aerobic conditions, pyruvate dehydrogenase (PD) is vital in the conversion of pyruvate to acetyl coA for the Krebs cycle (Patel & Korotchkina, 2006).

Multiple factors have the potential ability to control the intracellular glycolytic rate, including: rate limiting glycolytic enzymes (HK, PFK, PK) (Gropper & Smith; 2012), substrate availability, and the AMPK pathway. The influx of the main substrate for the glycolysis pathway, glucose, into the cell is mediated by facilitative glucose transporter (GLUT) proteins; part of the SLC2A family (Macheda et al, 2005). Glucose availability can also be managed via the regulation of glycogen storage in the muscle and liver and subsequent glucose resynthesis via glycogenesis and glycogenolysis respectively (Frayn, 2009). Lactate, pyruvate, glycerol and other amino acids can also be used as substrate for gluconeogenesis, predominantly in the liver, especially when muscle glycogen stores are low (often during exercise and starvation) (Exton, 1972). AMPK (5'-adenosine monophosphate activated kinase) also has long established roles in glycolytic regulation, especially during exercise and following blood glucose depletion (Hardie, 2007), with 12 distinct subunits each potentially fulfilling differing functions under various physiological conditions (Dasgupta & Chhipa, 2016). Within the glycolytic pathway, AMPK is believed to activate PFK, a rate-limiting glycolytic enzyme (Marsin et al, 2002). This, in turn, may aid in escalating the rate of glycolysis. In addition, activation of AMPK has exhibited a positive effect on the presence of GLUT proteins on the cell membrane; consequently, aiding glucose transport into the cell (Wu et al, 2013; Taylor et al, 2008; Stoppani et al, 2002; Holmes et al, 1999; Lee et al, 2006). Glycolysis is known to take place within the cytoplasm of the cell; hence the effectors are generally thought to reside intracellularly, but the hypothesis that ELVs may aid in mediating perturbations in glycolytic rate intercellularly is intriguing and requires further exploration. Understanding further intercellular mechanisms responsible for the maintenance of glycolytic metabolic homeostasis during exercise may aid understanding of the potential whole-body reaction to the energy demands of exercise and may have therapeutic potential in various metabolic conditions such as diabetes, and various glycolytic enzyme deficiencies.

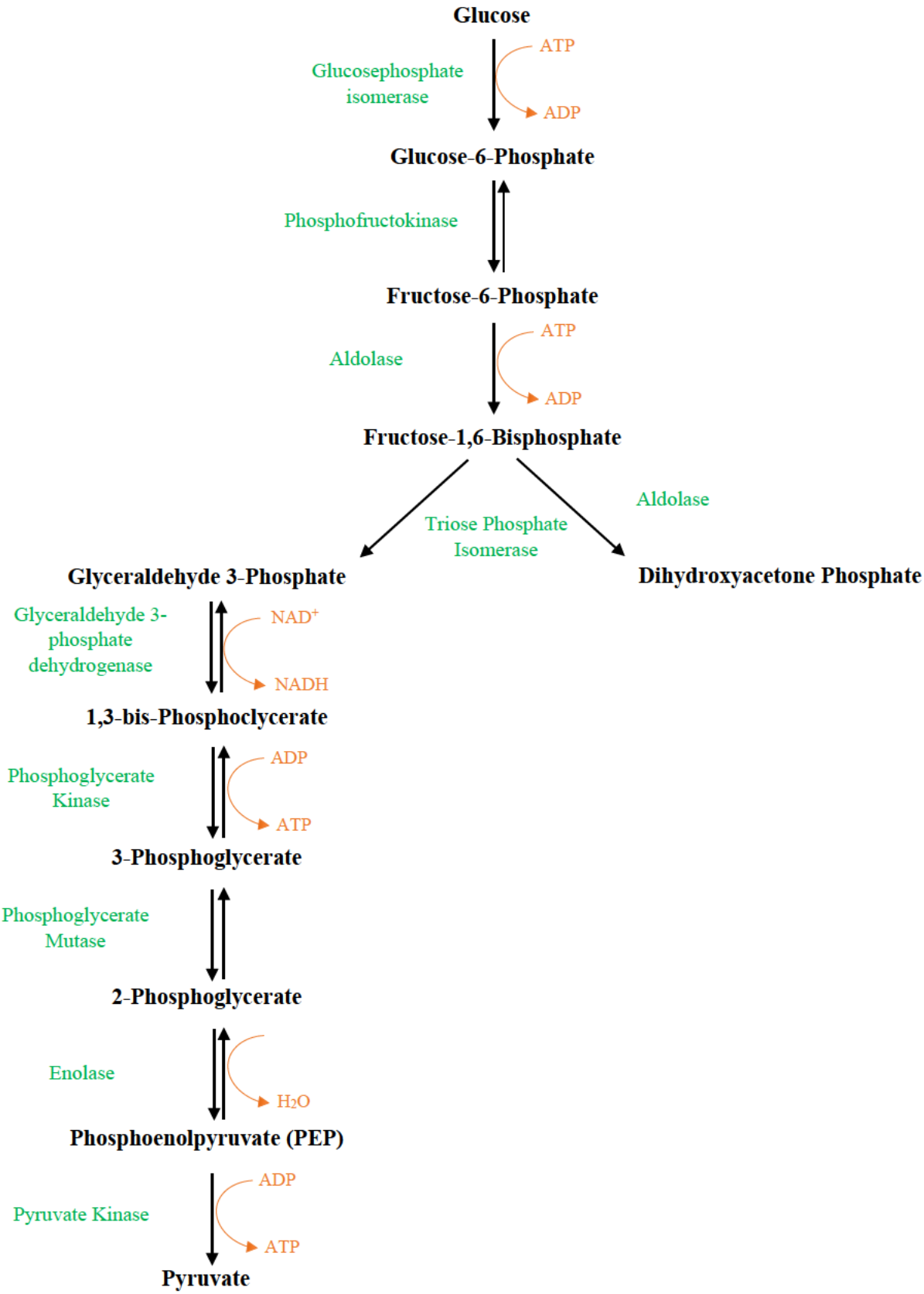


**Figure 2:** The glycolysis pathway and the relevant glycolytic enzymes involved.

## 1.6 ELVs and Glycolysis:

Unravelling the physiological relevance of the supposed exercise-mediated release of ELVs is a challenging yet potentially valuable task. In recent years there has been an emerging body of evidence advocating for a presence of multiple glycolytic enzymes in ELVs both in vivo (Whitham et al, 2018; Iliuk et al, 2020; Vanderboom et al, 2021) and in vitro (Jeppesen et al, 2019; Kugeratski et al, 2021; Garcia et al, 2015; Garcia et al, 2016). Moreover, and more importantly, there have more recently been observances that glycolytic enzymes in ELVs appear to be dynamically regulated by exercise (Whitham et al, 2018; Vanderboom et al, 2021), This was demonstrated in vivo by Whitham and colleagues (2018) with an observance of multiple 'proteins associated with glycolysis' in human plasma-derived ELVs isolated via UC (2 x 1-hour centrifugations at 20,000g at 4°C), confirmed via gene ontology enrichment proteomic analysis (more information at geneontology.org). Moreover, of the detected glycolytic enzymes (HK, GPI, PFK, GAPDH, PGK, ENO1, LDHA, LDHB, PK, PGM, TPI, ALDOA), 7 were shown to be significantly upregulated as a result of an exhaustive bout of cycling exercise (GAPDH; PGK; ENO1; LDHA; PK; TPI; ALDOA). However, this study utilised a fairly crude UC protocol, only deemed an intermediate specificity method at best (Théry et al, 2018); and it therefore remains possible that the results seen were simply contamination and not true ELV cargo. Much of this data appeared to be replicated in 2021 when Vanderboom and colleagues again reported a presence, and subsequent upregulation following exercise, of multiple glycolytic enzymes in human plasma-derived ELVs in their proteomic dataset (PGK1; ENO1; PKM; GAPDH; ALDOA; PGAM1; LDHA). In this study, ELVs were isolated via a protocol of SEC followed by UC. However, the group only utilised a single round of ultracentrifugation; differing to many modern studies which opted for two (such as: Whitham et al, 2018). Once again, this isolation protocol is deemed intermediate specificity at best in the MISEV guidelines (Théry

et al, 2018). This was followed by an alarming level of albumin in their proteomic dataset alluding to a high level of contamination in the ELV sample, as may be expected following the protocol utilised. These are the only studies to date to demonstrate a response to exercise of glycolytic enzymes in human plasma-derived ELVs, others have simply aimed to demonstrate their presence.

Iliuk and colleagues (2020) found a presence of many glycolytic enzymes in their proteomic dataset of healthy human plasma-derived ELVs, some common to Whitham et al (2018) (LDHA, ENO1, GAPDH, PGK1, ALDOA), and some novel (LDHB, PGAM4, HK1, PKM1, PKFP, GPI, PGM1). Interestingly, the same samples were also processed for phosphoproteomics in which many of the proteins present in the proteomic dataset were also detected in the ELVs as phosphorylated: GAPDH; PKM; PGM1; ENO1; ALDOA.

Alongside in vivo datasets, comprehensive in vitro studies have also demonstrated a presence of multiple glycolytic enzymes in ELV lysates. Kugeratski and colleagues (2021) showed, through proteomic analysis of ELV samples isolated via a single bout of UC from 14 different cell lines, that many glycolytic enzymes were present: GAPDH, PKFP, HK2, ENO2, PKM, HK1, PFKL, OGDH, GPI, ENO1, TPI1, PGK1, ALDOA, PGAM1. The cell used lines were all either fibroblast, pancreatic, kidney, lymphocyte, cancer, or hematopoietic (BJ, BxPC, HEK293, HPDE, HPNE, Jurkat, mCAF, MCF10A, MCF7, MDA-MB-231, PANC-1, PSC, Raji, THP-1). However, the single bout UC protocol at 100,000g is not thorough and is likely to have resulted in relatively high contamination in the sample. Therefore, in an attempt to overcome this caveat, the group also analysed datasets from 3 of the cell lines (HEK293T, PANC-1, MDA-MB-231) via multiple isolation methods (DG, importantly described as a ‘high specificity’ protocol in the MISEV guidelines (Théry et al, 2018), SEC, and UC) and found that all previously identified glycolytic enzymes were similarly present in all of these datasets, indicating a presence irrespective of chosen isolation

method. Importantly, the cargo proteome appeared consistent across isolation methods, and only distinctive between cell lines. ALDOA, PGAM1, GAPDH, LDHB, PKM, GPI, PGK1, ENO2, TPI1 and ENO1 were similarly reported to be present in ELVs isolated from human colon (DKO-1) and human glioblastoma cancer (Gli36) cell lines (Jeppesen et al, 2019). However, Jeppesen and colleagues (2019) described that following an isolation protocol of UC followed by DG, deemed to be a slightly higher specificity method (Théry et al, 2018), glycolytic enzymes were more abundant in the non-ELV fraction than the ELV fraction; creating some controversy in the field. Jeppesen and colleagues (2019) therefore hypothesised that the presence of glycolytic enzymes in ELV analyses are artefacts of unspecific isolation methods. However, as a counter criticism, since the ELVs in this study were collected from immortalised cell lines in the basal state, it may be expected that levels of glycolytic enzymes would be low in these ELV fractions as it has been shown that they are much more abundant following a metabolic stimulus (Whitham et al, 2018; Vanderboom et al, 2021). Also, since Jeppesen and colleagues (2019) only utilised 2 cell lines, according to Kugeratski and colleagues (2021), variance in the cargo proteome from other cell lines is to be expected, irrespective of isolation method. Moreover, none of the glycolytic proteins identified in the aforementioned proteomic datasets possessed a predicted signal sequence peptide suggestive of a classically secreted protein; insinuating that the proteins cannot conceivably exit a healthy cell in the absence of a vesicle.

Following such contradiction, it is imperative to assess the presence of glycolytic enzymes in ELVs using further specific methods. As a novel addition to this growing body of data, it would be valuable to assess the glycolytic enzyme content in muscle-derived ELVs; a highly dynamic, glycolytic and reactive tissue in response to metabolic stress.

## 1.7 Aims and Hypotheses:

The primary aim of the present study was to assess the presence of glycolytic enzymes in both murine muscle cell- and human plasma-derived ELVs, and to confirm previous proteomic data using a specific and targeted approach. Moreover, the present study aimed to assess whether the abundance of glycolytic enzymes in ELVs was responsive to metabolic stress in the context of both glucose availability and exercise. It was hypothesized that glycolytic enzymes would be present in both murine muscle cell- and plasma-derived ELVs and dynamically regulated by both glucose availability and exercise.

# 2. MATERIALS AND METHODS

## 2.1 Cell Lines and Culture:

A comprehensive list of all reagents and resources utilised is available in Table 2. Murine skeletal muscle C2C12 myoblast cells were seeded at a density of 2 million cells per 10cm tissue culture dish treated with Matrigel. For cell growth, DMEM was supplemented with: 1x GlutaMAX, 5mM glucose, 1mM sodium pyruvate, 10% (v/v) heat inactivated fetal bovine serum, and 1% (v/v) penicillin-streptomyocin (5000 units/mL-ug/mL). Differentiation of myoblasts into myotubes was undertaken at ~90% confluency using DMEM supplemented with: 1x GlutaMAX, either 5mM or 25mM glucose (dependent on experimental group), 1mM of sodium pyruvate, 2% (v/v) horse serum, and 1% (v/v) of penicillin-streptomyocin (5000 units/mL-ug/mL). Differentiation media was changed daily throughout. Prior to media collection for ELV isolation, cells were cultured in EV-depleted differentiation media for 48hrs commencing on day 7 of differentiation. For EV-depleted differentiation media, ELVs were depleted from horse serum via UC at 110000g overnight for 16 hours at 4°C using a S50-A fixed angle rotor in the Sorvall MTX 150 Micro-Ultracentrifuge (ThermoFisher Scientific, Leicestershire, UK). All cultures were maintained in a humidified incubator at 37°C, with a constant atmosphere of 95% air with 5% CO2.

Cells were counted using an automated cell counter (ThermoFisher Scientific, Leicestershire, UK). Cell viability was 100% on all counts measured using the automated cell counter following culture in EV-depleted media. Cell lysis was performed over ice using 10x rippa buffer. All samples were stored at -80°C prior to ELV isolation or analysis.

## 2.2 High Intensity Exercise Protocol:

*Participant Information.* The University of Birmingham STEM committee approved the ethics for the exercise protocol (code ERN_17-1570), and all practises were conducted in line with the Declaration of Helsinki. The study consisted of five young (mean age of 22.8 ± 5.2 years) and healthy participants (4 female, 1 male); defined by the Department of Health General Practise Physical Activity Questionnaire (2006). Mean VO2 peak across participants was 42.88 ml/kg/min and the average BMI was 23.3kg/$m^2$. Exclusion criteria included no history of cardiovascular, respiratory, metabolic, or neurological disease. All participants gave written, informed consent.

*Exercise Protocol.* Participants arrived at the laboratory fasted (no large meals 4 hours prior to arrival; no small meals 2 hours prior to arrival; no caffeine six hours prior to arrival; no alcohol 24 hours prior to arrival), well rested and hydrated, and having refrained from vigorous exercise 24 hours prior to testing. The initial screening visit comprised of a standardised incremental aerobic capacity protocol on a Lode cycle ergometer (Lode, Groningen, Netherlands) to determine both VO2 max (ml/kg/min) and Watt max; then used to determine the target intensity for the HIIT protocol in the subsequent visit. A Vyntus™ CPX Breath by Breath Metabolic Cart (Vyaire Medical, Mettawa, IL, USA), was used to measure VO2 max. In the subsequent visit, between 48 hours and two weeks following the initial visit, an 'all-out-HIIT' protocol was performed; 4x 30 second sprints on the Lode Bicycle Ergometer at 200% of Watt max with 4.5-minute active recovery between bouts. A warm up and cool down on the bicycle consisted of 10 minutes and 5 minutes respectively, both at a standard 50 Watts.

*Blood Handling.* Blood samples were collected in EDTA (ethylenediaminetetraacetic acid) tubes both 10 minutes pre the commencement and 30 seconds post the cessation of the

exercise protocol via an indwelling cannula in the antecubital vein. EDTA tubes both prevented coagulation of the plasma sample and removed calcium from the plasma; avoiding extra unwanted release of ELVs. Immediately following collection, samples were centrifuged twice for 15 minutes each at 2500g at room temperature with the aim to achieve platelet free plasma to be stored at -80°C prior to further isolation and analysis.

### 2.3 ELV Isolation:

C2C12 conditioned media was thawed at 4°C prior to ELV isolation via one of three methods UC, SEC, or IM.

*UC.* Preliminary centrifugation of thawed C2C12 conditioned media (400g for 10 minutes at room temperature; and subsequently 2000g for 20 minutes at 4°C) in the Sorvall Legend X1 centrifuge (ThermoFisher Scientific, Leicestershire, UK) preceded the ultracentrifugation protocol; to remove any remaining cell debris and particulate matter. The supernatant was retained following each centrifugation spin and the pellet was discarded. Following preliminary centrifugation, ELVs were isolated from the supernatant via 2 rounds of ultracentrifugation at 110000g for 2 hours each at 4°C in S50-A and S55-A2 fixed angle rotors respectively in the Sorvall MTX 150 Micro-Ultracentrifuge (ThermoFisher Scientific, Leicestershire, UK). After the first, the supernatant was collected (non-ELV fraction) and the vesicle pellet was resuspended in ice-cold PBS in preparation for the second round of ultracentrifugation; after which the supernatant was discarded and ELV pellets lysed in 1x Tris-SDS buffer (20mM Tris-HCl and 2% (w/w) SDS). The non-ELV fraction was lysed in 5x Tris-SDS buffer (100mM Tris-HCl and 10% (w/w) SDS) and all samples were sonicated for 6 rounds of 30 seconds at 4°C each to ensure complete solubility in the Bioruptor Plus Sonication System (Diagenode, Liege, Belgium).

*SEC.* Thawed C2C12 conditioned media was concentrated via centrifugation in Amcon Ultra-15 filters (Merck Life Sciences, Darmstadt, Germany), at 4000g for 10 minutes at room temperature with a molecular weight cut-off at 100kDa. 5ml of concentrated culture media was loaded into a qEV10 column with porous, polysaccharide resin (Izon, Oxford, UK). Each column was used a maximum of 5 times and was flushed with 60ml 0.5M NaOH and 120ml filtered PBS between samples to avoid cross contamination. Columns were only reused with samples of consistent biological origins to further avoid cross contamination. For each vesicle sample 7 fractions of 500µl each were collected using the Automated Fraction Collector (Izon, Oxford, UK). Fractions 1-3 (deemed by the official user manual to contain the ELVs) were pooled to maximise protein yield for downstream analysis. Each fraction was further concentrated via centrifugation in Amcon Ultra-15 filters at 4000g for 30 minutes at room temperature and subsequently lysed in 5x Tris-SDS buffer prior to sonication for 6 rounds of 30 seconds each at 4°C each to ensure complete solubility in the Bioruptor Plus Sonication System.

*IM.* Immunomagnetic isolation was performed using the EasySep™ Human Pan-Extracellular Vesicle Positive Selection Kit and "The Big Easy" (StemCell Technologies, Vancouver, Canada) magnet to isolate CD9-, CD63-, and CD81-positive ELVs as per manufacturer's instructions. Upon thawing, plasma samples were centrifuged at 5000g for 10 minutes at 4°C with the aim to remove large vesicles. 6ml plasma was then added to the Selection Cocktail, mixed and incubated for 10 minutes at room temperature. Releasable RapidSpheres were added to the sample and then incubated for a further 10 minutes at room temperature. PBS was added to the sample to top it up to 10ml before the tube was placed into the magnet and incubated for 5 minutes at room temperature. The supernatant was discarded and the sample was washed with PBS a further 3 times. Finally, the tube was removed from the magnet and isolated ELVs were lysed in 1x Tris-SDS, buffer prior to

centrifugation at 5000g for 5 minutes at room temperature to extract beads and leave the lysed ELV sample in the supernatant. The sample was finally sonicated for 6 rounds of 30 seconds each at 4°C to ensure complete solubility.

### 2.4 Sample Preparation and Western Blot:

Total protein was established using the DC (detergent compatible) colorimetric protein assay. BSA (bovine serum albumin) protein standards were utilised to create a standard curve for each assay and subsequently used to determine the total protein content of each sample. BSA standards were prepared in 5x Tris-SDS lysis buffer at concentrations of 0, 0.125, 0.25, 0.5, 1, 2 µg/µl. Absorbance was read at a wavelength of 750nM using a filter-based multi-mode microplate reader (BMG Labtech, Offenburg, Germany). Samples were subsequently prepared at equal protein concentrations for Western Blot in 1x NuPAGE LSD sample buffer containing 2-mercaptoethanol (final concentration 1.5%) and left at room temperature to denature overnight before storage at -80°C prior to subsequent analysis. Cell lysate samples and samples isolated via UC were prepared at 1 µg/µl, and samples isolated via SEC and immunomagnetic isolation were prepared at 0.3µg/µl.

Prepared samples were loaded into 10% Bis/Tris gels poured in-house in preparation for SDS-PAGE (sodium dodecyl sulfate-polyacrylamide gel electrophoresis). Loaded gels were placed in 1x MOPS SDS running buffer for 10 minutes at 100V and a subsequent 50 minutes at 150V. Proteins were then transferred onto PVDF (polyvinylidene diflouride) membranes in 1 x Transfer Buffer (48mM Tris-HCl, 39mM glycine; 10% (v/v) methanol) for 60 minutes at 100V. Membranes were blocked in a solution of 5% milk powder in TBS-T (Tris-buffered saline Tween-20) for approximately 60 minutes, and subsequently incubated overnight at 4°C with the corresponding primary antibody (detailed in Table 1). The following morning,

membranes were washed three times with TBS-T for 5 minutes each time, prior to incubation in the secondary antibody (detailed in Table 1) for 60 minutes at room temperature. Since all primary antibodies used were rabbit-derived, an anti-rabbit IgG secondary antibody was used in all cases. The membranes were then washed with TBS-T three further times for 5 minutes each prior to incubation in ECL (electrochemiluminescence) for 2 minutes. Imaging was completed using a G:BOX Chemi-XR5 (Syngene, Cambridgeshire, UK) and quantification using ImageJ software.

### 2.5 ExoView™:

Plasma samples were analysed using the ExoView™ Cargo Kit Assay (NanoView Biosciences, Boston, MA, USA) as per the instructions in the official manual. Plasma samples were first diluted in the incubation solution (1:100). ExoView™ chips were placed face-up in the centre of each well using tweezers; avoiding contact with the central area of the chip containing the antibodies (as detailed in Table 1). 35µl of the diluted plasma sample was then pipetted onto the chip prior to the overnight incubation of the plate. Following the incubation, 1ml of wash solution was added to each well and the plate was shaken on a microplate shaker at 500rpm for 3 minutes. 750µl was then removed and the chips were then washed as per the instructions in the manual. The bound ELVs underwent a permeabilization step to allow cargo to be probed and then washed a further 3 times. Fluorescently labelled antibodies were prepared in blocking solution (as detailed in Table 1). 250ul of pooled cargo blocking solution was placed in each well. Plate was incubated for an hour in the dark at room temperature prior to further wash steps: 3 with Solution A; 3 with Solution B; 1 with deionised water (all following the same protocol as previous wash steps). Following the washing process, chips were transferred using tweezers to a 10cm dish containing the rinse

solution. Again, caution was taken not to touch the central part of the chip (containing the antibodies) with the tweezers, so as not to disturb the antibodies. After washing the chips gently in the rinse solution, they were extracted using tweezers and placed face up on absorbent paper to dry. The chips were then placed into the ExoView™ reader to generate fluorescent spot images.

| Antibody | Source | Manufacturer | Catalogue # | Dilution |
|---|---|---|---|---|
| *Western Blot* | | | | |
| GAPDH | Rabbit | Cell Signalling Technology | #5174 | 1:1000 |
| CD9 | Rabbit | Abcam | #ab92726 | 1:1000 |
| PGK1 | Rabbit | Abcam | #ab199438 | 1:2000 |
| PKM2 | Rabbit | Cell Signalling Technology | #4053 | 1:1000 |
| PGAM1 | Rabbit | Cell Signalling Technology | #12098 | 1:1000 |
| PKM1/2 | Rabbit | Cell Signalling Technology | #3190 | 1:1000 |
| Hexokinase II | Rabbit | Cell Signalling Technology | #2867 | 1:1000 |
| Pyruvate Dehydrogenase | Rabbit | Cell Signalling Technology | #7074 | 1:1000 |
| Syntenin 1 | Rabbit | Abcam | #ab19903 | 1:1000 |
| Alix | Rabbit | Abcam | #ab186429 | 1:1000 |
| TSG101 | Rabbit | Abcam | #ab125011 | 1:1000 |
| Albumin | Rabbit | Cell Signalling Technology | #4929 | 1:1000 |
| Anti-rabbit IgG | Goat | Cell Signalling Technology | #7074 | 1:1000 |
| *ExoView™* | | | | |
| CD9 | | | | 1:500 |
| CD63 | | | | 1:500 |
| CD81 | | | | 1:500 |
| Recombinant Alexa Fluor 555 Anti-GAPDH | Rabbit | Abcam | #ab206629 | 1:200 |

**Table 1:** Antibody Details

## 2.6 Glucose and Lactate Assays:

Total glucose in C2C12 myotube cell culture media was measured using a bioluminescent Glucose Assay Kit (Promega, Madison, WI, USA). Glucose was measured at 0-, 24-, and 48-hour timepoints in both the LG and HG conditions. Glucose standards were used to formulate a standard curve. The process was repeated on the same samples using a bioluminescent Lactate Assay Kit (Promega, Madison, WI, USA) to measure lactate in the media against a set of lactate standards. Results were read using a filter-based multi-mode microplate reader.

## 2.7 Statistical Analysis:

Statistical analysis was performed, in all cases, using GraphPad Software Inc Prism version 9. An unpaired two-tailed t-test investigated significant differences in protein expression between LG and HG C2C12 myotube-derived ELV samples isolated via UC ($\alpha$=0.05). In instances where variance was significantly different between conditions ($p<0.05$), determined with an F test, Welch's correction was used. Data are presented as mean ± standard deviation, with individual data points on the graph. A paired two-tailed t-test was employed to detect significant differences in protein expression in human plasma-derived ELV samples pre and post exercise isolated via immunomagnetic isolation ($\alpha$=0.05). Data is presented as individual paired data points. Power was calculated using the DSS (Decision Support Systems) 'Statistical Power Calculator Using Average Values' Power Calculator using a 5% alpha confidence level and 20% beta confidence level. Cohen's D effect size was calculated for significant values ($p<0.05$). To assess any significant differences in glucose and lactate assay values between LG and HG conditions and time bathing in media, a factorial 2 condition (LG, HG) x 3 time point (0hr, 24hr, 48hr) ANOVA with Tukey's correction was used. Results are reported as individual data points.

## 2.8 EV Track:

All practices were carried out as close to the MISEV 2018 guidelines as possible (Théry et al, 2018). Furthermore, EV Track (Van Deun et al, 2017), an online resource metric used to encourage method reproducibility was implemented, and an estimate score of 78% has been generated for the study as a whole based on the EV Track reported core elements, as depicted in Figure 3. The average score in 2021 is currently only 53% across 75 studies, leaving the present study well above average. EV Track aims to create a standardisation of agreed method protocols in EV research, that may eliminate much of the variability that is currently seen and encourage reproducibility of studies, using informed experimental parameters.

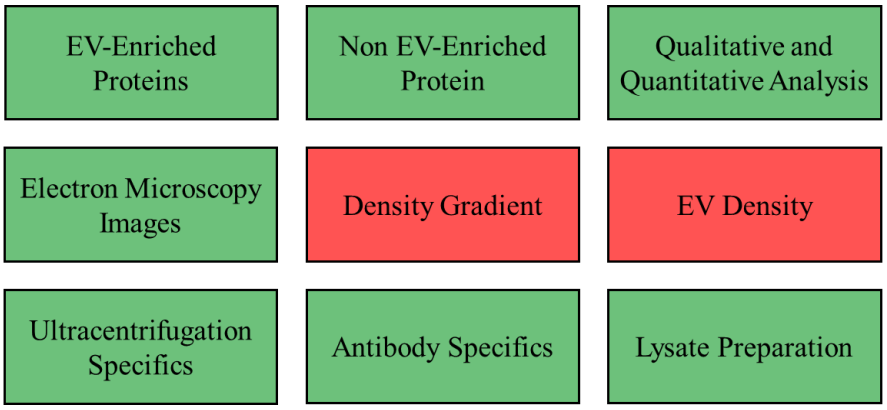


**Figure 3:** Nine core elements of EV Track. Green denotes that the element has been achieved in the present study and red denotes that it has not been possible.

| Reagent or Resource | Source | Identifier |
|---|---|---|
| *Cell Culture:* | | |
| C2C12 Myoblasts | American Type Culture Collection | CRL-1772 |
| T75 Tissue Culture Treated Flasks | VWR International | 734-2313 |
| 10cm Tissue Culture Treated Dishes | Scientific Laboratory Supplies Ltd | G664160 |
| Matrigel | ThermoFisher Scientific Ltd | 11573560 |
| DMEM | ThermoFisher Scientific Ltd | 11520416 |
| Glutamax | ThermoFisher Scientific Ltd | 35050061 |
| Glucose | Merck Life Sciences Ltd | G7528 |
| Sodium Pyruvate | Merck Life Sciences Ltd | S8636 |
| Fetal Bovine Serum Heat Inactivated | Merck Life Sciences Ltd | F9665 |
| Penicillin-streptomyocin | ThermoFisher Scientific Ltd | 11528876 |
| Horse Serum Heat Inactivated | ThermoFisher Scientific Ltd | 10368902 |
| Ethanol | ThermoFisher Scientific Ltd | 10000652 |
| Rippa Buffer | Scientific Laboratory Supplies Ltd | 20-188 |
| Automated Cell Counter | ThermoFisher Scientific Ltd | AMQAF1000 |
| *High Intensity Exercise Protocol:* | | |
| Lode Cycle Ergometer | Lode | 960900 |
| Vyntus™ CPX Breath by Breath Metabolic Cart | Vyaire Medical | |
| Cannula | Becton Dickinson | 391452 |
| EDTA Tubes | Becton Dickinson | VS367838 |
| *Extracellular Vesicle Isolation:* | | |
| Sorvall Legend X1 Centrifuge Series | ThermoFisher Scientific Ltd | 10036894 |

| | | |
|---|---|---|
| Sorvall MTX 150 Micro-Ultracentrifuge | ThermoFisher Scientific Ltd | 46960 |
| PBS | ThermoFisher Scientific Ltd | 12549079 |
| SDS | VWR International | A1112.0500 |
| Bioruptor Plus Sonicator System | Diagenode | B01020001 |
| Automatic Fraction Collector | IZON | |
| Amcon Ultra-15 Filters | Merck Life Sciences | UFC910024 |
| qEV10 | IZON | SP3 |
| NaOH | Merck Life Sciences | 655104 |
| EasySep™ Human Pan-Extracellular Vesicle Positive Selection Kit | StemCell Technologies | 17891 |
| The Big Easy | StemCell Technologies | 18001 |
| Optiprep Density Gradient Medium | Merck Life Sciences | D1556 |
| ExoView™ | NanoView Biosciences | |
| ExoView™ Cargo Kit | NanoView Biosciences | |
| *Sample Preparation and Western Blot:* | | |
| DC Assay | Bio-Rad Laboratories Ltd | 5000111 |
| BSA | Fisher Scientific Ltd | 12881630 |
| FLUOstar Omega filter-based multi-mode microplate reader | BMG Labtech | |
| 1x NuPAGE LDS | ThermoFisher Scientific Ltd | 11559166 |
| 2-mercaptoethanol | ThermoFisher Scientific Ltd | 10306050 |
| Bis-Tris | VWR International | 6976-37-0 |
| 40% Acrylamide | ThermoFisher Scientific Ltd | 10001313 |

| | | |
|---|---|---|
| TEMED | Merck Life Sciences | T7024 |
| APS | Merck Life Sciences | A3678 |
| MOPS-SDS Running Buffer | ThermoFisher Scientific Ltd | NP0001 |
| Tris-HCl | ThermoFisher Scientific Ltd | 10724344 |
| Glycine | VWR International | A1067.5000 |
| Tween | VWR International | 9005-64-5 |
| Methanol | ThermoFisher Scientific Ltd | 11976961 |
| NaCl | ThermoFisher Scientific Ltd | 746398 |
| PVDF Membrane | Scientific Laboratory Supplies Ltd | 10600021 |
| ECL | ThermoFisher Scientific Ltd | 11556345 |
| G Box Chemi XR5 | Syngene | |
| *Glucose and Lactate Assays:* | | |
| Glucose-Glu Assay Kit | Promega | J6021 |
| Lactate-Glo Assay Kit | Promega | J5021 |
| Image J | https://imagej.nih.gov/ij/ | |
| *Statistical Analysis:* | | |
| GraphPad Software Inc Prism version 9 | | |
| DSS 'Statistical Power Calculator with Average Values' | https://www.dssresearch.com/resources/calculators/statistical-power-calculator-average/ | |

***Table 2:*** *Reagent and Resource Details*

# 3. RESULTS

## 3.1 C2C12 Myotubes in Culture Release ELVs:

Following the isolation of C2C12 myotube-derived ELVs via either UC or SEC, common ELV marker proteins were used to indicate the efficacy of the isolation. In the absence of a gold standard ELV isolation method, as discussed, it has here been attempted to use multiple ELV isolation methods where possible to negate the conclusion that findings are simply an artefact of the ELV isolation approach. Western Blots confirmed the presence of traditional putative exosome markers CD9, Syntenin-1, ALIX and TSG101 (Kowal et al, 2016) in each ELV lysate isolated via both UC (Figure 4a) and SEC (Figure 4b). ELV lysates were deemed to be F1-3 following SEC isolation as per the official user manual. Meanwhile, such markers were either not detectable or very lowly expressed in the non-ELV lysates (Figure 4a) or non-ELV fractions (Figure 4b) (F4-7), implying that, in agreement with the MISEV guidelines (Théry et al, 2018), the chosen methods were effective at isolating the vast majority of the ELV population, but are not absolute. Results were consistent across the lysates from all three biological replicates (each a pool of multiple technical replicates from three separate cell passages). Following SEC isolation, albumin (largely considered to be a contaminant in ELV lysates) was exclusively detected in fractions 6 and 7, deemed to be non-EV fractions; further validating the success of the isolation. There were small amounts of albumin detected in ELV samples following UC isolation, as may have been expected since it is only deemed an intermediate specificity method (Théry et al, 2018). Cell viability was recorded at 100% on all counts. The findings so far validate that the isolation methods utilised were appropriate to examine C2C12 myotube-derived ELV content.

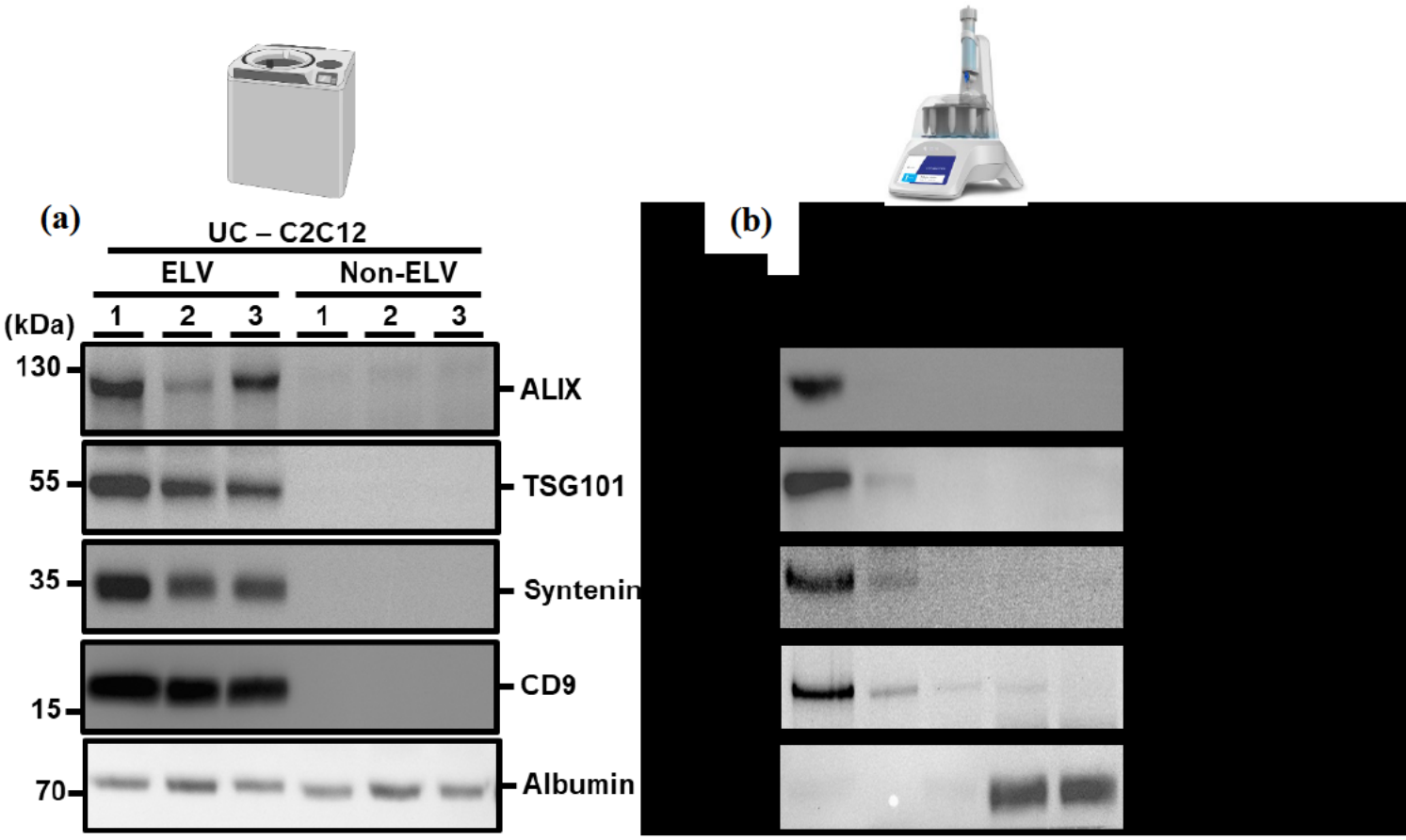


**Figure 4**: **C2C12 Myotubes in Culture Release EVs.** Western Blots confirmed the presence of multiple common ELV marker proteins in C2C12 myotube-derived ELV lysates following both UC (a) and SEC (b) isolation. Representative images shown for 3 distinct biological replicates of each sample.

### 3.2 C2C12 Myotube-Derived ELVs Contain Glycolytic Enzymes:

Following confirmation that the chosen ELV isolation methods were appropriate, the lysates were further analysed via Western Blot to test the hypothesis that glycolytic enzymes are present in C2C12 myotube-derived ELVs. In all three biological replicates isolated via UC, 7 glycolytic enzymes were detected in the ELV lysates; HK II; PKM2; PKM1/2; PGK1; PD; GAPDH; PGAM1 (Figure 5a). The majority were not detectable in the non-ELV lysates, other than PKM2, PKM1/2 and PD which were detectable but very lowly expressed in the non-ELV fractions; potentially explained by the low expression of some of the ELV markers in these lysates (Figure 4a) and therefore the fact that the ELV isolation may not have been completely effective. Western Blot analysis of fractions 1-7 following SEC isolation (Figure 5b) demonstrated a replication of the finding that glycolytic enzymes HKII, PGK1, GAPDH, and PGAM1 are present in murine muscle cell-derived ELV lysates (SEC F1-3). Though some glycolytic enzymes were also detected in the later fractions (deemed to be non-ELV), the expression was very low throughout; concurrent with some of the ELV markers (Figure 4b). Cell viability was recorded at 100% on all counts. Overall, these finding validate that ELVs isolated from C2C12 conditioned media contain a variety of glycolytic enzymes, supporting the hypothesis.

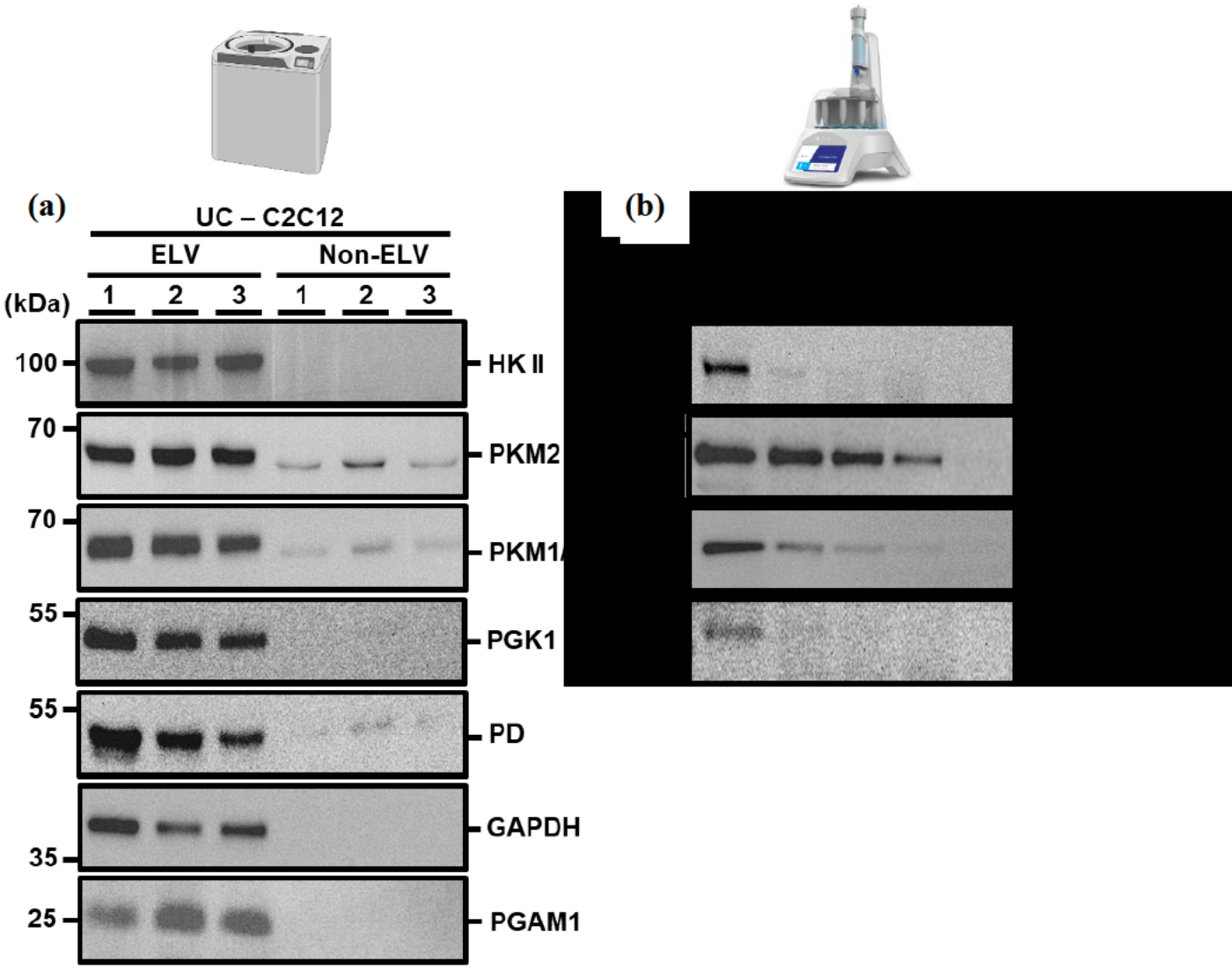


**Figure 5: C2C12 Myotube-Derived ELVs Contain Glycolytic Enzymes.** Western Blots confirmed the presence of multiple glycolytic enzymes in C2C12 myotube-derived ELV lysates following both UC (a) and SEC (b) isolation. Representative images shown for 3 distinct biological replicates of each sample.

### 3.3 Glucose availability Alters the Abundance of Glycolytic Enzymes in C2C12 Myotube-Derived ELVs:

Following the detection of multiple glycolytic enzymes in C2C12 myotube-derived ELV lysates, and confirmation that UC was an appropriate isolation method, an in vitro model of glucose availability manipulation was designed to address the hypothesis that glycolytic enzyme expression would be dynamically regulated by glucose availability in C2C12 myotube-derived ELVs. As depicted in Figure 6a, differences in glucose availability and cellular metabolic stress between LG and HG were confirmed via glucose and lactate assays at varying timepoints. A two-way factorial ANOVA with Tukey's correction revealed a significant main effect of both glucose condition ($F(1, 6) = 807.2$, $p< 0.0001$.) and time the cells were bathing in the media ($F(2, 6) = 387.9$, $p<0.0001$), with a significant interaction effect ($F(2, 6) = 144.3$, $p>0.0001$) on glucose assay results. This confirms that cells in the LG and HG condition were exposed to significantly different levels of glucose. Similarly, depicted in Figure 6b, a two-way factorial ANOVA revealed a significant main effect of both glucose condition ($F(1, 6) = 28.26$, $p= 0.0018$.) and time the cells were bathing in the media ($F(2, 6) = 121.2$, $p<0.0001$), with a significant interaction effect ($F(2, 6) = 29.39$, $p=0.0008$) on lactate assay results. At the 48hr timepoint, lactate concentration was significantly upregulated in the HG condition compared to the LG condition ($p=0.0007$). This reveals that metabolic rates were significantly different between the LG and the HG conditions, and point towards higher metabolic stress in the LG conditions. The results of the two assays together confirm that the model was successful at altering glucose availability in the cells. Figure 6d depicts representative Western Blot images and subsequent quantifications of three distinct biological replicates (each a pool of technical replicates) derived from C2C12 myotubes cultured in LG or HG enriched media. An unpaired t-test revealed a significant upregulation of 5 of the glycolytic enzymes in the LG condition compared to the HG condition: GAPDH

(p=0.0003), PGK1 (p=0.0409), PKM1/2 (p=0.0379), PKM2 (0.0476), and PD (p=0.0099). Despite the small sample size, the effect sizes as calculated by Cohen's D were very high in all cases (11.3, 4.70, 4.61, 2.83, and 4.61 respectively). On the other hand, expression of both HKII and PGAM1 did not change with significance between ELV samples from the LG and HG conditions (p=0.0673 and p=0.1252 respectively). Cell viability was recorded at 100% on all counts. These findings overall advocate for a role of limited glucose availability in dynamically regulating the expression of glycolytic enzymes in ELVs derived from C2C12 myotube cells, supporting the hypothesis.

**(a)**

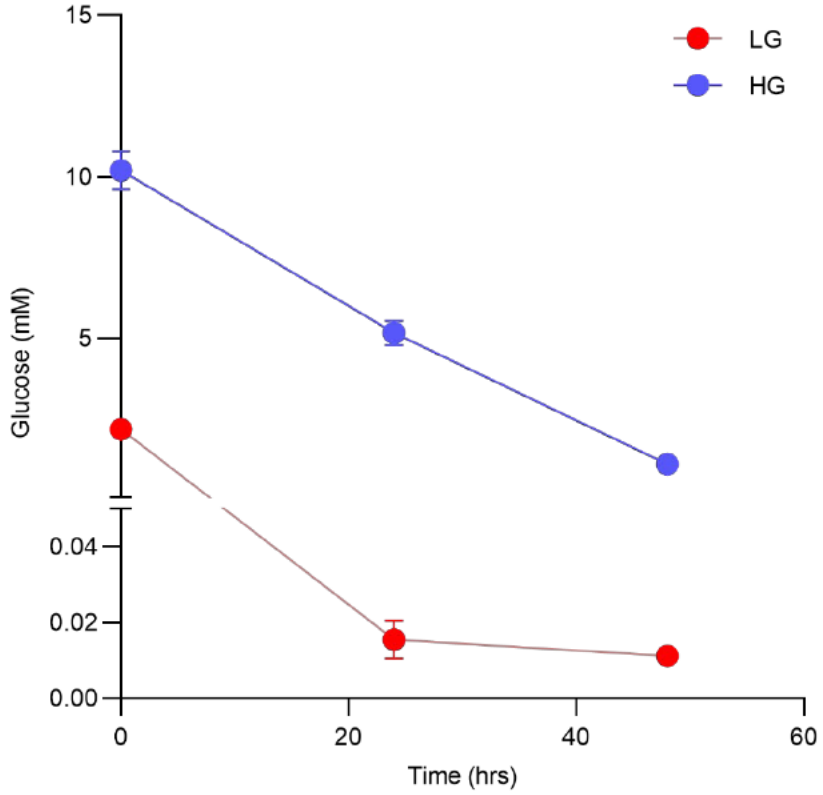
LG
HG
Glucose (mM)
15
10
5
0.04
0.02
0.00
0
20
40
60
Time (hrs)

**(b)**

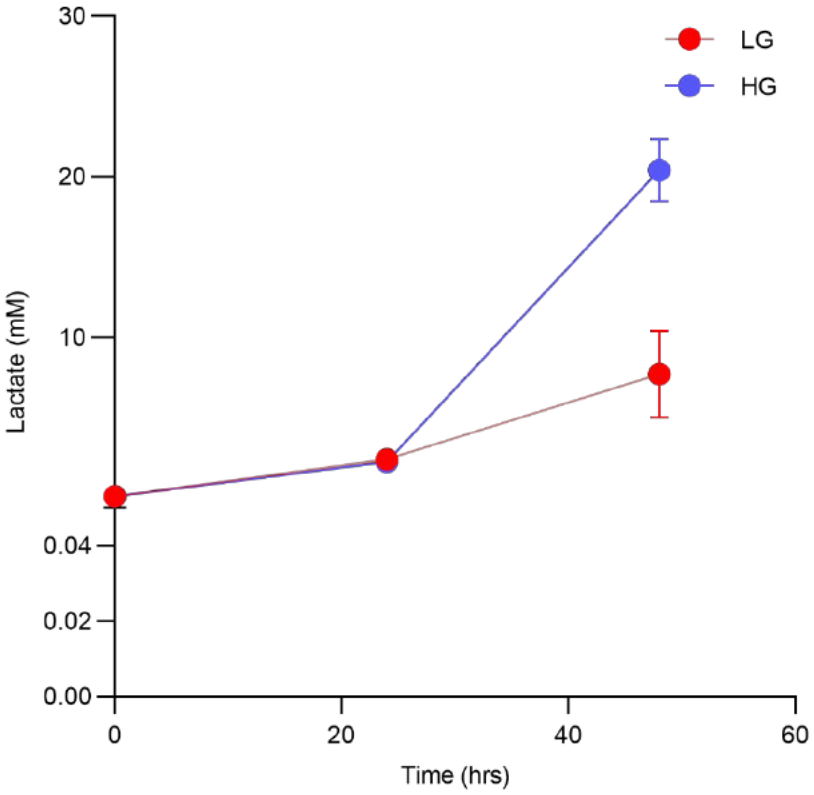
LG
HG
Lactate (mM)
30
20
10
0.04
0.02
0.00
0
20
40
60
Time (hrs)

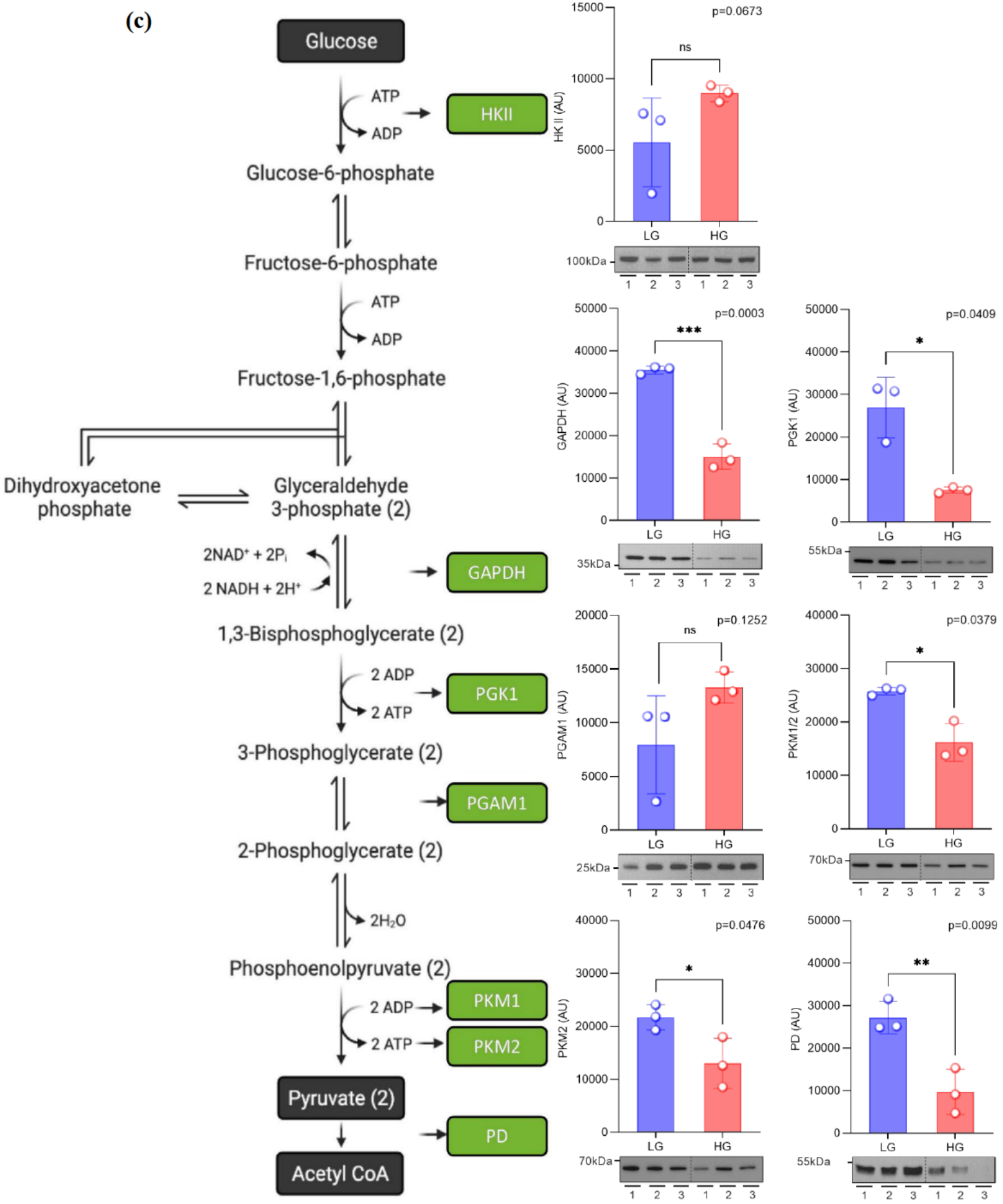


**Figure 6: Glucose availability Alters the Abundance of Glycolytic Enzymes in C2C12 Myotube-Derived ELVs.** Glucose (a) and lactate (b) assays confirmed higher energy stress in the LG condition compared to HG. Western Blots and subsequent unpaired t-tests confirmed significantly greater expression of GAPDH, PGK1, PKM1/2, PKM2 and PD in the LG condition compared to HG (c). Results reported as mean ± standard deviation with individual data points.

### 3.4 Alterations in Glycolytic Enzyme Content of ELVs are Independent of Cellular Changes:

Alterations in the abundance of ELV cargo proteins, as seen in the present study in the context of glycolytic enzymes, have previously been cited as simply reflections of the protein content of the parent cell (Zhao et al, 2016). To test this, the lysed C2C12 cells from the LG and HG conditions were analysed via Western Blot for the same glycolytic targets as the ELV lysates (Figure 7a). Cell viability on all counts was recorded as 100%. Following quantification, an unpaired t-test revealed no significant upregulation of multiple of the glycolytic enzymes seen to change in the ELV samples between LG and HG conditions: GAPDH ($p=0.4925$), PGK1 ($p=0.2837$), and PKM2 (0.3448). PKM1/2 and PD were both significantly upregulated in the HG conditions in the cell lysates, the opposite trend to the ELV samples ($p=0.0191$ and $p=0.0431$ respectively) (Figure 7a). Unlike the ELV lysates, in the cell lysates expression of HKII was significantly upregulated in the LG condition ($p=0.0062$) and expression of PGAM1 was significantly upregulated in the HG condition ($p=0.0335$). The patterns in the expression of glycolytic enzymes in the ELVs were therefore independent of the changes occurring in the cell as trends were not replicated.

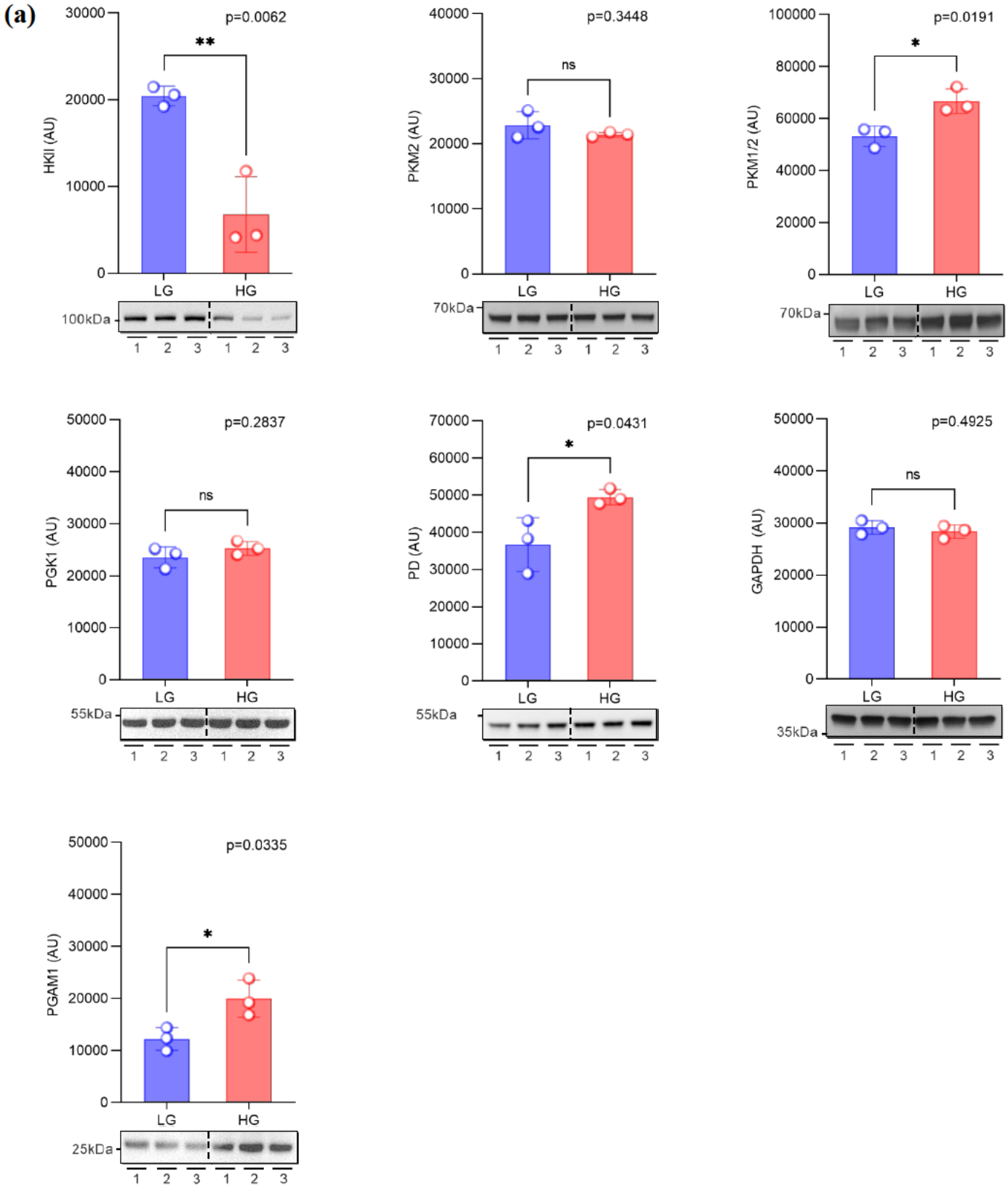


**Figure 7: Alterations in Glycolytic Enzyme Content of ELVs are Independent of Cellular Changes.**

Representative Western Blot images and subsequent unpaired t-tests revealed a significant increase in the expression of HKII in the LG condition compared to the HG (p=0.0260) (a). PKM1/2 was significantly upregulated in the HG condition (p=0.05). Results reported as mean ± standard deviation with individual data points. *p<0.05.

### 3.5 Human Plasma-Derived ELVs Contain Glycolytic Enzymes:

Mindful of the hypothesis that glycolytic enzymes are simply an artefact of ELV isolation (Jeppesen et al, 2019), plasma samples from young healthy participants in a rested state were analysed via an immunoaffinity based nanofluidic assessment at single EV resolution to assess the presence of GAPDH as cargo in CD9-, CD63- AND CD81-positive ELVs; no prior ELV isolation of the sample required. Tetraspanins CD9, CD63 and CD81 have all been shown to be putative universal exosome markers (Kowal et al, 2016), hence the choice.

The ExoView™ instrument detected fluorescence emitted from the GAPDH conjugated green Alexaflor555 antibody in CD9, CD63 and CD81 positive immobilised ELVs. This provides clear evidence, at a single EV resolution, that GAPDH is present in ELVs circulating in human plasma (Figures 8b, 8c, 8d). No GAPDH was detected on the mouse IgG control spot, as expected (Figure 8a). The detection of GAPDH seen here therefore adds support to the hypothesis that glycolytic enzymes are not only packaged in ELVs derived from C2C12 myotubes cells in vitro but also appear in circulation in vivo.

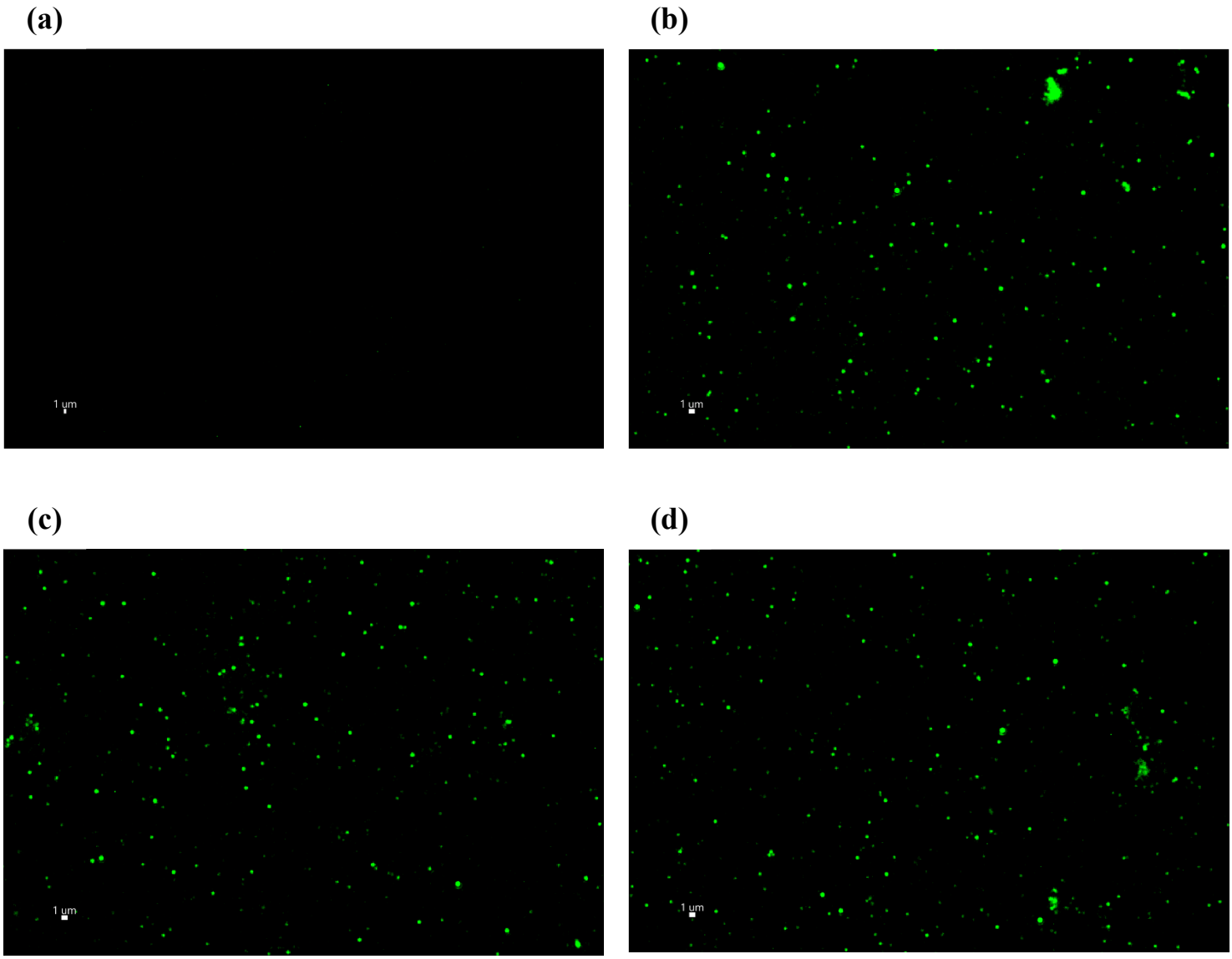


**Figure 8: Human Plasma-Derived ELVs Contain Glycolytic Enzymes.** Capture spots from ExoView chips of healthy human plasma. Panel a shows a control capture mouse IgG capture spot. Other panels show green fluorescence emitted from an Alexaflour555 anti-GAPDH recombinant antibody on a CD9 capture spot (b), a CD63 capture spot (c), and a CD81 capture spot (d).

### 3.6 High Intensity Exercise Alters the Abundance of Glycolytic Enzymes in Human Plasma-Derived ELVs:

Limited glucose availability and exercise share many common pathways. In light of the observed effect of differing glucose availability on dynamic regulation of the glycolytic enzyme content of myotube-derived ELVs, it has here been hypothesised that an exhaustive bout of exercise might also alter glycolytic content of ELVs in circulation in vivo. A model of high intensity exercise was used to determine whether exercise had an effect on ELV release into the circulation, and whether the abundance of glycolytic enzymes in the ELVs was altered as a result. Following demonstration via ExoView™ that GAPDH is present in tetraspanin-positive ELVs in vivo, a similar means of immobilisation was used to examine if GAPDH presence is dynamic in response to exercise. The isolation method utilised was a highly sensitive immunomagnetic protocol that similarly captures CD9-, CD63-, and CD81-positive ELVs. As can be seen in Figure 9a, Western blots and subsequent paired t-test revealed a significant upregulation of CD9 and GAPDH expression post exercise ($p=0.0211$ and $p=0.0141$ respectively), with high effect sizes as calculated by Cohen's D (2.07 and 1.51 respectively). There were no significant changes from pre to post exercise in ALIX ($p=0.1191$), TSG101 ($p=0.1739$), HKII ($p=0.0534$). Mindful of a potential lack of power, the DSS power calculator revealed, however, that with the addition of just one more participant the power of HKII would have been over 80%, and would therefore have been likely to be significant (5% alpha confidence level and 20% beta confidence level). These findings further suggest a role of exercise, in dynamically regulating expression of glycolytic enzymes in human plasma-derived ELVs, supporting the hypothesis.

**( a)**

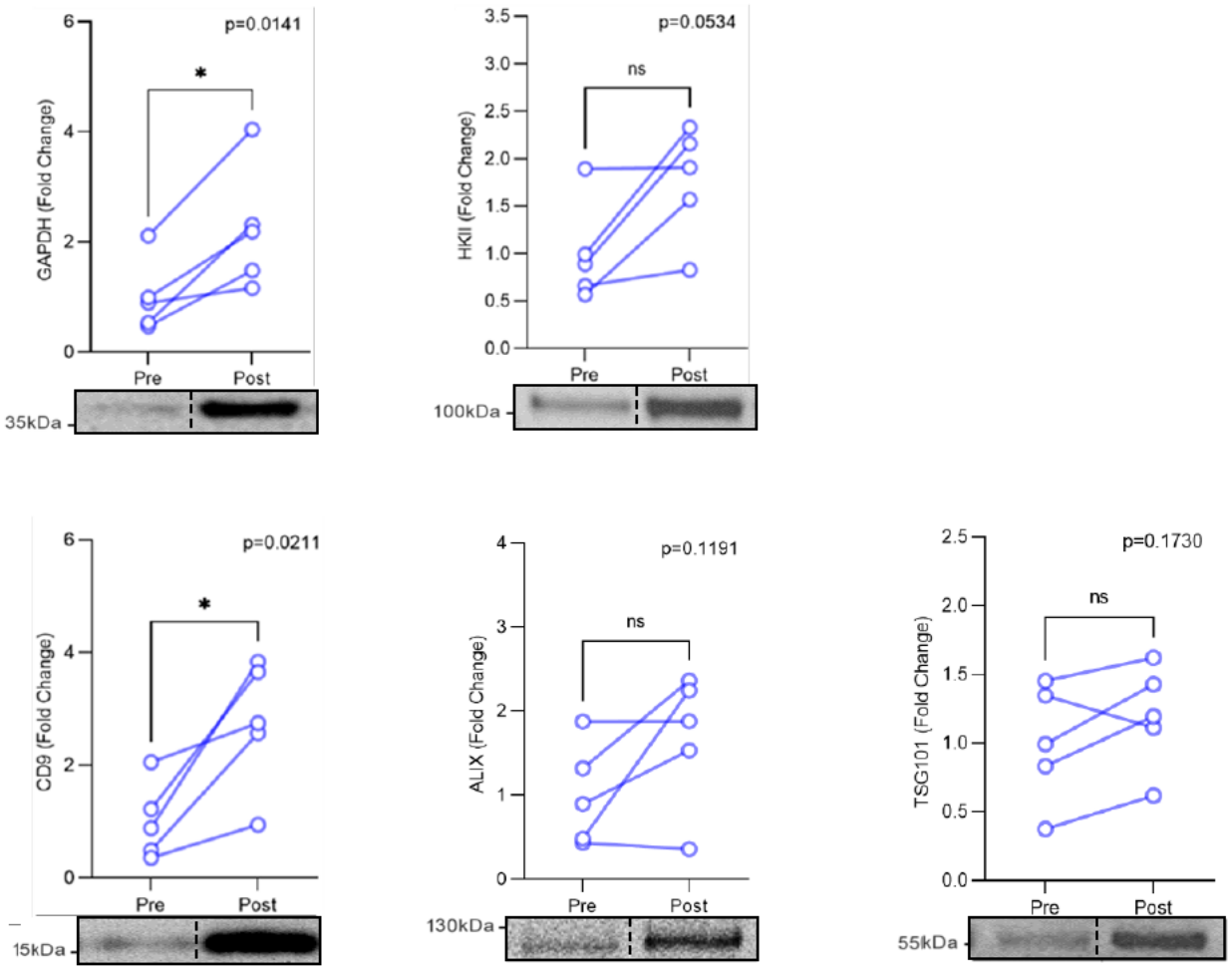


**Figure 9: High Intensity Exercise Alters the Expression of Glycolytic Enzymes in Human Plasma-Derived ELVs.** Representative Western Blot images and subsequent quantifications and paired t-tests (a) revealed a significant increase in the expression of CD9 and GAPDH in ELV' samples isolated via BigEasy following high intensity exercise. *p<0.05. **p<0.01.

# 4. DISCUSSION

## 4.1 Summary:

Previous attempts to underpin the cargo proteome of exercise-mediated ELVs, and therefore begin to understand their physiological relevance, have unexpectedly revealed a presence, and response to exercise, of multiple glycolytic enzymes in ELVs (Whitham et al, 2018; Vanderboom et al, 2021). However, the physiological function of glycolytic enzymes in this context remains unclear, and some data contradicts this finding; reporting that glycolytic enzymes may only be present in ELVs as an artefact of the chosen isolation methods (Jeppesen et al, 2019), a common concern in the EV field. Using multiple specific methods supported by the MISEV guidelines (Théry et al, 2018), the present study utilised both in vitro and in vivo models to provide a confirmation that glycolytic enzymes are detected in both murine muscle cell- and human plasma-derived ELVs, irrespective of isolation method; supporting the hypothesis. Moreover, suitable highly specific and targeted methods were used to demonstrate that the expression of many glycolytic enzymes appears to be responsive to, and dynamically regulated by, glucose availability in vitro and exercise in vivo, once again supporting the hypothesis.

## 4.2 Glycolytic Enzymes in ELVs:

As hypothesised, one of the largest contributors to the maintenance of metabolic homeostasis and dynamic regulation of glycolysis during exercise, skeletal muscle, has here been shown in vitro to release ELVs containing multiple glycolytic enzymes as detected by western blot following both standard UC and SEC isolation protocols. In the absence of a

gold standard isolation method, the use of multiple methods here can add weight to the findings (Théry et al, 2018). Though this was only shown here in a singular cell line, it uses a targeted method that adds to a body of work demonstrating a presence of common proteins (except PD) in 14 other non-muscle cell lines and via multiple ELV isolation methods (Kugeratski et al, 2021). Though the expression of some glycolytic enzymes did not appear exclusive to the ELV fractions (Figure 5a; Figure 5b), nor was expression of some putative ELV markers (Figure 4a; Figure 4b). This implies that this may merely be a limitation of the ELV isolation method, especially since the methods are only described as intermediate recovery (Théry et al, 2018), implying that some ELVs may remain in the non-ELV fractions. Since the observed glycolytic enzymes are not known to possess signal peptides, it is difficult to reconcile their presence in the extracellular environment in the absence of either cell death or a vesicle. Figures 4a, 4b, 5a, and 5b collectively demonstrate that glycolytic enzymes may be co-expressed in ELVs with syntenin-1. Since sytenin-1 has been recently described as the most abundant putative universal ELV marker (Kugeratski et al, 2021), the apparent finding that multiple glycolytic enzymes may be present in syntenin-1 positive ELVs is encouraging.

Following confirmation in vitro, the present study also corroborates and builds on previous findings (Whitham et al, 2018; Iliuk et al, 2020; Vanderboom et al, 2021) by demonstrating a presence of various glycolytic enzymes in human plasma-derived tetraspanin-positive ELVs following highly specific immunomagnetic isolation and immunoaffinity capture using the ExoView™ (Figures 8b, 8c, 8d, and 9a). These tetraspanins have previously been shown to increase in circulation with exercise and are therefore deemed to be appropriate markers with which to study exercise-mediated ELVs (Brahmer et al, 2019). The ExoView™ is a highly sensitive immunoaffinity capture method that analyses at a single EV resolution level, and importantly negates the requirement for ELV isolation, and subsequently the bias and contamination this may carry. Furthermore, IM isolation has been

deemed by the MISEV guidelines as more specific and effective at isolating ELVs than DG (Théry et al, 2018); the method used by Jeppesen and colleagues (2019) when they hypothesised that glycolytic enzymes are only detected in ELVs as an artefact of the isolation method. This provides encouragement that glycolytic enzymes are present in ELVs irrespective of isolation method, supporting the hypothesis.

Though Jeppesen and colleagues (2019) discussed that glycolytic enzymes may simply be present in ELV samples as an artefact of the chosen isolation method, the results of the present study combined with data from Kugeratski and colleagues (2021) promotes the hypothesis that isolation method has very limited effect on the ELV cargo proteome observed. Since Jeppesen and colleagues (2019) used only two cell lines, which were both cancer cell lines, it could be conceivable that this is the reason for the low expression of some of the glycolytic enzymes seen in previous studies in their ELV samples. Further, the use of ExoView™ here to demonstrate the presence on GAPDH in ELVs in vivo negates the requirement for isolation altogether (Figure 8b, 8c, 8d). This corroborates the recent supposition that GAPDH may be a putative universal ELV marker (Kugeratski et al, 2021). The present study therefore provides validation of and builds on a somewhat convincing body of work demonstrating a presence of multiple glycolytic enzymes in ELVs from multiple sample types (Garcia et al, 2016; Whitham et al, 2018; Iliuk et al, 2020; Kugeratski et al, 2021; Vanderboom et al, 2021).

### 4.3 Glycolytic Enzymes in ELVs are Responsive to Glucose Availability and High Intensity Exercise:

The finding that glycolytic enzymes are present in ELVs in vitro and in vivo is intriguing, yet not conclusive evidence to show that ELVs have a function in increasing

glycolytic rate during exercise. Of further interest to the exercise field is the notion that the expression of glycolytic enzymes in ELVs in vivo and in vitro is dynamically responsive to perturbations in metabolic stress (Whitham et al, 2018; Vanderboom et al, 2021). Here, we show that GAPDH, PGK1, PKM2, PKM1/2, and PD appeared more abundantly in ELV lysates from myotubes in the LG condition compared to HG condition following UC isolation (Figure 6d), previously shown to be an appropriate isolation method to study C2C12 myotube-derived ELVs (Figure 4a). The expression of HKII and PGAM1, however, did not change significantly between glucose availability conditions. Intriguingly, both proteins appeared to trend in the opposite direction; a slight upregulation in ELVs isolated from the HG conditions. However, both datasets were significantly underpowered, (63.7% and 65.9% respectively) making it near impossible to draw conclusions from these observations. In vivo, exercise here stimulated the release of immunomagnetically isolated CD9-, CD63- and CD81-positive ELVs enriched with GAPDH and HKII (Figure 9a). This corroborates the ExoView data in the present study demonstrating a presence of GAPDH in CD9-, CD63-, and CD81-positive ELV (Figure 8b, 8c, 8d). The increase in CD9-positive ELVs following exercise shown via Western Blot (Figure 9a) both confirms the validity of the immunomagnetic isolation and is consistent with previous findings (Brahmer et al, 2019). This finding that the glycolytic enzyme content in ELVs is responsive to metabolic stress may also partially explain why Jeppesen and colleagues (2019), who analysed ELV samples from cells in the basal state, only observed low glycolytic enzyme content.

### 4.4 The Functional Relevance of Glycolytic Enzymes in ELVs:

This data overall advocates for a role of exercise-mediated ELVs in transporting glycolytic enzymes and therefore potentially aiding the glycolytic response to exercise via the

horizontal transfer of glycolytic enzymes between cells and tissues. There has been limited yet valuable functional evidence to demonstrate that ELVs carrying glycolytic enzymes have the ability to alter glycolytic rate in the target tissue. Garcia et al (2016) showed a positive correlation between glucose starvation of cultured cardiomyocytes (CMs) and CD63-positive-vesicle release containing GAPDH, LDH, GLUT1 and GLUT4. GLUT 1 and GLUT4 were demonstrated to be transferred to cerebral microvascular endothelial cells (CMVEC) via live imaging. As a probable effect of this transfer, glucose uptake was significantly increased in the CMVEC, independent of a direct physiological stressor in the CMVEC. However, the CM and CMVEC tissues are anatomically close in the body and communication and diffusion between the tissues is long established; with the performance of each modulating the performance of the other (Brutsaert, 2013; Brutsaert et al, 1998; Brzezinka et al, 2005). Therefore, whilst this data is intriguing, it may not be representative of the crosstalk that ELVs are potentially capable of. Other work demonstrating an altered glycolytic rate following culture with ELVs is in the context of cancer: bone marrow stromal cells demonstrated increased glycolytic rate when cultured with leukemic extracellular vesicles (Johnson et al, 2016); and prostate cancer cells demonstrated increased glycolytic rate when cultured with ELVs from cancer-associated fibroblast cells (Zhao et al, 2016). Since ELVs appear to have the ability to alter metabolism in a pathological state, it is conceivable that this function may be extended to wider physiological states, such as exercise. Finally, though not in the context of glycolysis, the potential for ELVs to alter metabolism in the target cell has also been demonstrated in lipogenesis: Sano and colleagues (2014) described an effect of hypoxic adipocyte-derived ELVs on lipogenesis in 3T3-L1 cells in culture. Moreover, a major criticism of the supposition that ELVs transferring metabolic enzymes can alter the metabolic rate in the target tissue is that cells already contain an abundance of such enzymes; a very small amount deposited from ELVs will surely not affect

the rate. However, this criticism was addressed by Park and colleagues (2005) who stated that even a very small increase in G6PD (glucose-6-phosphate dehydrogenase) (as seen in exosomes by Sano and colleagues (2014)) has been reported to promote lipogenesis in 3T3-L1 cells, albeit in vitro.

Though conclusions regarding the function of glycolytic enzymes in ELVs in the present study cannot be made, the findings that they are responsive to exercise (Whitham et al, 2018; Vanderboom et al, 2021) promote a non-random selection process by which glycolytic enzymes are packaged into exercise-mediated ELVs. It may therefore be hypothesised that there is some physiological relevance underpinning their release and transportation in ELVs during exercise and that they could conceivably be delivered to a target cell or tissue to increase glycolytic rate. The detection of HKII in ELVs in vitro and in vivo in the present study (Figure 5a, 5b, 9a), a major rate limiting glycolytic enzyme, may be of importance as should the ELVs be capable of transferring this protein to other cells and tissues, as have previously been described in various contexts (Montecalvo et al, 2012; Tian et al, 2013; Mulcahy et al, 2014; Garcia et al, 2016), HKII may have the ability to directly alter the glycolytic rate in the target cell or tissue.

A further intriguing hypothesis is the notion that glycolytic enzymes may be partitioned into ELV's for the purpose of mediating active metabolism within the vesicle itself. The present study, along with previous work (Garcia et al, 2015; Garcia et al, 2016; Whitham et al, 2018; Jeppesen et al, 2019; Iliuk et al, 2020; Vanderboom et al, 2021; Kugeratski et al, 2021;) would indicate that much of the machinery required for glycolysis is present in ELV's, yet it remains unknown whether they may act as independent units capable of glycolysis. Should this be the case and ELV's are able to produce, and deliver to cells, substrates required for various steps of glycolysis, the rate limiting steps of glycolysis may indeed be bypassed in the cell. This may therefore enable an increase in glycolytic rate in the

cell beyond the limitations of the abundance of the rate limiting enzymes and their relevant substrates. Though this has not yet been investigated in the context of glycolysis, Iraci and colleagues (2017) described that ELVs have the potential to act as independent, metabolically active units capable of functional L-asparaginase activity in the microenvironment via Asrg11 (Iraci et al, 2017), providing encouragement to the early supposition that this may also be the case in the context of glycolysis.

However, recent work appears to insinuate a larger role of GAPDH in ELVs; stating that it may in fact be an ELV surface protein with a function in ELV biogenesis (Dar et al, 2021). Though this is intriguing, it does not rule out the supposition that GAPDH and other glycolytic enzymes have a function in mediating alterations in glycolytic rate via ELVs, especially in response to exercise.

### 4.5 ELV Cargo Changes Independent of Cellular Changes:

It has previously been suggested that the cargo proteome of ELVs is simply a reflection of the conditions and proteome of the parent cell (Zhao et al, 2016) and that therefore in this case, alterations in glycolytic enzymes expression in C2C12 myotube-derived ELV lysates in response to metabolic stress would be replicated in the cell lysates. However, findings here may suggest that this is not the case. The alterations in expression of glycolytic enzymes seen here in C2C12 myotube-derived ELVs (Figure 6c) do not appear to be replicated in the cell lysates (Figure 7a). The finding that ELV cargo, specifically related to glycolysis, is dynamic in response to a metabolic stimulus irrespective of changes in the parent cell proteome may further support the suggestion that there is a complex physiological reason behind their selective packaging beyond simply a reflection of the parent cell. However, one consideration to be made is that when assessing the expression of glycolytic

enzymes in cell lysates, the abundance may be so high that differences between conditions are masked. Although, as can be seen in Figure 7a, there are in fact significant differences in expression of some of the glycolytic enzymes between the LG and HG conditions in the cell lysates, therefore suggesting that differences are not being masked by universal high expression.

### 4.6 Therapeutic Potential:

The weight of evidence supporting a role of ELVs in transporting glycolytic enzymes (Garcia et al, 2016; Jeppesen et al, 2019; Iliuk et al, 2020; Kugeratski et al 2021), with response to both glucose availability and exercise (Whitham et al, 2018; Vanderboom et al, 2021), as corroborated in the present study, appears to suggest a potential role of exercise-induced ELVs in maintaining metabolic homeostasis via tissue crosstalk. Muscle cells have here been illustrated as a potential origin of such vesicles. In therapeutic terms, the proposed characterisation of metabolically active enzymes in ELVs may have therapeutic potential in patients lacking these enzymes. Whitham and colleagues (2018) demonstrated that exercise-mediated ELVs appeared to gravitate towards liver cells; especially if they carried the marker ITGB5. It is therefore conceivable that many of the exercise-mediated ELVs seen in the present study may also demonstrate tropism to the liver and therefore act as couriers of glycolytic enzymes to the liver. It may therefore be proposed that exercise mediated ELVs may become a treatment for liver-presenting enzyme deficiencies, such as pyruvate dehydrogenase deficiency, which can cause hyperammonaemia, hypotonia, lethargy and seizures, among other side effects (Kerr et al, 1988; Wexler et al, 1992). This hypothesis that ELVs may be used as targeted drug therapies, bypassing a significant immune response and subsequent side effects, is of high importance to the field (Johnsen et al, 2014). Many early

yet successful attempts have utilised ELVs in this way (Peinado et al, 2012; Jang et al, 2013; Bose et al, 2018), with clinical trials ongoing (as described in Hermann et al, 2021). Much of this work has utilised the loading of specific proteins into ELVs either exogenously or endogenously (Vader et al, 2016) and subsequently delivering them to target cells or tissues both in vitro (such as: Alvarez-Elviti et al, 2011; Mentkowski et al, 2019) and in vivo (such as: Tian et al, 2014; Gupta et al, 2021). However, such engineered ELVs have often shown signs of protein degradation (Hung & Leonard, 2015). Therefore, should natural exercise-mediated ELVs enriched with glycolytic enzymes prove an effective therapy, this barrier will be overcome. Assessing the effect of glycolytic enzyme enriched ELVs on a target cell or tissue will aid in further determining the subsequent therapeutic potential of exercise-mediated ELVs enriched with glycolytic enzymes.

## 4.7 Limitations and Future Directions:

One major limitation of the present study is the sole use of the immortalised C2C12 cell line. Although the C2C12 line is widely used and accepted, it is highly glycolytic and more representative of type II myotubes. In order to get a more comprehensive view of the potential role of ELVs in glycolysis, similar investigations in human primary muscle fibres obtained from more oxidative muscles may compliment the current work. The present study began to negate the criticism that glycolytic enzymes may be contaminants in ELV samples introduced by crude isolation methods by utilising multiple, thorough isolation methods and even the ExoView™; removing the requirement for ELV isolation altogether. However, in order to make this data conclusive, all glycolytic enzymes would need to be detected via the ExoView™ method. In addition to the glycolytic enzymes analysed in the present study, it may also be of interest to investigate the potential ELV content of other proteins involved in

glucose metabolism such as GLUT proteins. GLUT1 and GLUT4 were demonstrated by Garcia and colleagues (2016) to be present in ELVs via Western Blot, but confirmation via the ExoView™ and subsequent analysis of regulation via glucose availability and exercise would add to the findings of the present study. Moreover, since the tetraspanins used have occasionally been shown to be non-exclusive to exosomes, other more specific proposed exosomes markers such as Syntenin-1, ALIX, and TSG101 may be of more value in order to capture the exosomes on the ExoView™ chips (Kugeratski et al, 2021). Though it cannot yet be guaranteed that using alternative markers would solely result in exosome detection (and not other vesicles subpopulations), it may aid in getting closer to this goal. Furthermore, an assessment of glycolytic enzymes content in exosomes using the ExoView™ to show their potential response to exercise and glucose availability in vivo would be of great value, and would further build on the results shown here with a highly specific method. Moreover, since the amount of glycolytic enzymes that can be carried in ELVs is much smaller than what appears to be present in the target cell already, it is imperative to carry out a functional study to decipher the metabolic impact of glycolytic enzyme delivery by ELVs. In vivo, in order to increase the power of the present findings a higher sample number would be useful and insightful. Finally, though this study gained a relatively high EV Track (Van Deun et al, 2017) score of 78%, in order to raise this score and therefore raise the reliability of the results within the EV field, density gradient and subsequent measures of EV density would need to be employed.

## 4.8 Conclusions:

To conclude, these data demonstrate that glycolytic enzymes are detected in murine muscle cell-derived ELVs in vitro, irrespective of isolation method and are responsive to

glucose availability, as hypothesised. Furthermore, glycolytic enzymes GAPDH and HKII are detected in tetraspanin-positive ELVs in human plasma and are increased in circulation in response to a high intensity exercise bout, as hypothesised, with confirmation of GAPDH presence using the highly specific ExoView™.

# 5. REFERENCE LIST


Alvarez-Erviti, L., Seow, Y., Yin, H., Betts, C., Lakhal, S. and Wood, M.J., 2011. Delivery of siRNA to the mouse brain by systemic injection of targeted exosomes. *Nature Biotechnology,* 29(4), pp.341-345.

Baietti, M.F., Zhang, Z., Mortier, E., Melchior, A., Degeest, G., Geeraerts, A., Ivarsson, Y., Depoortere, F., Coomans, C., Vermeiren, E. Zimmermann, P., and David, G., 2012. Syndecan–syntenin–ALIX regulates the biogenesis of exosomes. *Nature cell biology*, 14(7), pp.677-685.

Barra, N.G., Chew, M.V., Holloway, A.C. and Ashkar, A.A., 2012. Interleukin-15 treatment improves glucose homeostasis and insulin sensitivity in obese mice. *Diabetes,* Obesity and Metabolism, 14(2), pp.190-193.

Berditchevski, F. and Odintsova, E., 2007. Tetraspanins as regulators of protein trafficking. *Traffic*, 8(2), pp.89-96.

Brahmer, A., Neuberger, E., Esch-Heisser, L., Haller, N., Jorgensen, M.M., Baek, R., Möbius, W., Simon, P. and Krämer-Albers, E.M., 2019. Platelets, endothelial cells and leukocytes contribute to the exercise-triggered release of extracellular vesicles into the circulation. *Journal of Extracellular Vesicles,* 8(1), p.1615820.

Brennan, K., Martin, K., FitzGerald, S.P., O'Sullivan, J., Wu, Y., Blanco, A., Richardson, C. and Mc Gee, M.M., 2020. A comparison of methods for the isolation and separation of extracellular vesicles from protein and lipid particles in human serum. *Scientific Reports,* 10(1), pp.1-13.

Brutsaert, D.L., 2003. Cardiac endothelial-myocardial signaling: its role in cardiac growth, contractile performance, and rhythmicity. *Physiological Reviews,* 83(1), pp.59-115.

Brutsaert, D.L., Fransen, P., Andries, L.J., De Keulenaer, G.W. and Sys, S.U., 1998. Cardiac endothelium and myocardial function. *Cardiovascular Research,* 38(2), pp.281-290.

Brzezinska, A.K., Merkus, D. and Chilian, W.M., 2005. Metabolic communication from cardiac myocytes to vascular endothelial cells. *American Journal of Physiology-Heart and Circulatory Physiology,* 288(5), pp.H2232-H2237.

Busquets, S., Figueras, M., Almendro, V., López-Soriano, F.J. and Argilés, J.M., 2006. Interleukin-15 increases glucose uptake in skeletal muscle. An antidiabetogenic effect of the cytokine. *Biochimica et Biophysica Acta (BBA)-General Subjects,* 1760(11), pp.1613-1617.

Cocozza, F., Grisard, E., Martin-Jaular, L., Mathieu, M. and Théry, C., 2020. SnapShot: extracellular vesicles. *Cell,* 182(1), pp.262-262.

Colombo, M., Raposo, G. and Théry, C., 2014. Biogenesis, secretion, and intercellular interactions of exosomes and other extracellular vesicles. *Annual Review of Cell and Developmental Biology*, 30, pp.255-289.

Dar, G.H., Mendes, C.C., Kuan, W.L., Speciale, A.A., Conceição, M., Görgens, A., Uliyakina, I., Lobo, M.J., Lim, W.F., El Andaloussi, S., Mäger, I., Roberts T.C., Barker R.A., Goberdhan D.C.I., Wilson C., and Wood M.J.A., 2021. GAPDH controls extracellular vesicle biogenesis and enhances the therapeutic potential of EV mediated siRNA delivery to the brain. *Nature Communications,* 12(1), pp.1-15.

Dasgupta, B. and Chhipa, R.R., 2016. Evolving lessons on the complex role of AMPK in normal physiology and cancer. *Trends in Pharmacological Sciences,* 37(3), pp.192-206.

Exton, J.H., 1972. Gluconeogenesis. *Metabolism,* 21(10), pp.945-990.

Farhana, A. and Lappin, S.L., 2020. Biochemistry, Lactate Dehydrogenase. StatPearls. Treasure Island (FL): *StatPearls Publishing*.

Febbraio, M.A., Hiscock, N., Sacchetti, M., Fischer, C.P. and Pedersen, B.K., 2004. Interleukin-6 is a novel factor mediating glucose homeostasis during skeletal muscle contraction. *Diabetes,* 53(7), pp.1643-1648.

Frayn, K.N., 2009. Metabolic regulation: a human perspective. *John Wiley & Sons*.

Frühbeis, C., Helmig, S., Tug, S., Simon, P. and Krämer-Albers, E.M., 2015. Physical exercise induces rapid release of small extracellular vesicles into the circulation. *Journal of Extracellular Vesicles*, 4(1), p.28239.

Garcia, N.A., Ontoria-Oviedo, I., González-King, H., Diez-Juan, A. and Sepúlveda, P., 2015. Glucose starvation in cardiomyocytes enhances exosome secretion and promotes angiogenesis in endothelial cells. *PloS One*, 10(9), p.e0138849.

Garcia, N.A., Moncayo-Arlandi, J., Sepulveda, P. and Diez-Juan, A., 2016. Cardiomyocyte exosomes regulate glycolytic flux in endothelium by direct transfer of GLUT transporters and glycolytic enzymes. *Cardiovascular Research*, 109(3), pp.397-408.

Goldstein, M.S., 1961. Humoral nature of the hypoglycemic factor of muscular work. *Diabetes,* 10, pp.232-234.

Gonzales, P.A., Pisitkun, T., Hoffert, J.D., Tchapyjnikov, D., Star, R.A., Kleta, R., Wang, N.S. and Knepper, M.A., 2009. Large-scale proteomics and phosphoproteomics of urinary exosomes. *Journal of the American Society of Nephrology,* 20(2), pp.363-379.

Gropper, S.S. and Smith, J.L., 2012. Advanced nutrition and human metabolism. *Cengage Learning*.

Hansen, J., Brandt, C., Nielsen, A.R., Hojman, P., Whitham, M., Febbraio, M.A., Pedersen, B.K. and Plomgaard, P., 2011. Exercise induces a marked increase in plasma follistatin: evidence that follistatin is a contraction-induced hepatokine. *Endocrinology,* 152(1), pp.164-171.

Hardie, D.G., 2007. AMPK and SNF1: snuffing out stress. *Cell Metabolism,* 6(5), pp.339-340.

Harding, C., Heuser, J. and Stahl, P., 1983. Receptor-mediated endocytosis of transferrin and recycling of the transferrin receptor in rat reticulocytes. *The Journal of Cell Biology*, 97(2), pp.329-339.

Holmes, B.F., Kurth-Kraczek, E.J. and Winder, W.W., 1999. Chronic activation of 5′-AMP-activated protein kinase increases GLUT-4, hexokinase, and glycogen in muscle. *Journal of Applied Physiology*, 87(5), pp.1990-1995.

Hondares, E., Iglesias, R., Giralt, A., Gonzalez, F.J., Giralt, M., Mampel, T. and Villarroya, F., 2011. Thermogenic activation induces FGF21 expression and release in brown adipose tissue. *Journal of Biological Chemistry,* 286(15), pp.12983-12990.

Hsu, C., Morohashi, Y., Yoshimura, S.I., Manrique-Hoyos, N., Jung, S., Lauterbach, M.A., Bakhti, M., Grønborg, M., Möbius, W., Rhee, J., Barr, F.A. and Simons M., 2010. Regulation of exosome secretion by Rab35 and its GTPase-activating proteins TBC1D10A–C. *Journal of Cell Biology*, 189(2), pp.223-232.

Hung, M.E. and Leonard, J.N., 2015. Stabilization of exosome-targeting peptides via engineered glycosylation. *Journal of Biological Chemistry,* 290(13), pp.8166-8172.

Iliuk, A., Wu, X., Li, L., Sun, J., Hadisurya, M., Boris, R.S. and Tao, W.A., 2020. Plasma-derived extracellular vesicle phosphoproteomics through chemical affinity purification. *Journal of Proteome Research,* 19(7), pp.2563-2574.

Iraci, N., Gaude, E., Leonardi, T., Costa, A.S., Cossetti, C., Peruzzotti-Jametti, L., Bernstock, J.D., Saini, H.K., Gelati, M., Vescovi, A.L., Bastos, C., Faria N., Occipinti L.G., Enright A.J., Frezza C. and Pluchino S., 2017. Extracellular vesicles are independent metabolic units with asparaginase activity. *Nature Chemical Biology*, 13(9), p.951.

Jeppesen, D.K., Fenix, A.M., Franklin, J.L., Higginbotham, J.N., Zhang, Q., Zimmerman, L.J., Liebler, D.C., Ping, J., Liu, Q., Evans, R., Fissell, W.H., Patton J.G., Rome L.H., Burnette D.T. and Coffey R.J., 2019. Reassessment of exosome composition. *Cell*, 177(2), pp.428-445.

Johnson, S.M., Dempsey, C., Chadwick, A., Harrison, S., Liu, J., Di, Y., McGinn, O.J., Fiorillo, M., Sotgia, F., Lisanti, M.P., Parihar, M., Krishnan S. and Saha V., 2016. Metabolic reprogramming of bone marrow stromal cells by leukemic extracellular vesicles in acute lymphoblastic leukemia. *Blood, The Journal of the American Society of Hematology,* 128(3), pp.453-456.

Johnstone, R.M., Adam, M., Hammond, J.R., Orr, L. and Turbide, C., 1987. Vesicle formation during reticulocyte maturation. Association of plasma membrane activities with released vesicles (exosomes). *Journal of Biological Chemistry*, 262(19), pp.9412-9420.

Kalra, H., Simpson, R.J., Ji, H., Aikawa, E., Altevogt, P., Askenase, P., Bond, V.C., Borràs, F.E., Breakefield, X., Budnik, V., Buzas, E., Camussi G., Clayton A., Cocucci E., Falcon-Perez J.M., Gabrielsson S., Gho Y.S., Gupta D., Harsha H.C., Hendrix A., Hill A.F., Inal J.M., Jenster G., Krämer-Albers E., Lim S.K., Llorente A., Lötvall J., Marcilla

A., Mincheva-Nilsson L., Nazarenko I., Nieuwland R., Nolte-'t Hoen E.N.M., Pandey A., Patel T., Piper M.G., Pluchino S., Prasad T.S.K., Rajendran L., Raposo G., Record M., Reid G.E., Sánchez-Madrid F., Schiffelers R.M., Siljander P., Stensballe A., Stoorvogel W., Taylor D., Thery C., Valadi H., van Balkom B.W.M., Vázquez J., Vidal M., Wauben M.H.M., Yáñez-Mó M., ZoellerM. and Mathivanan S., 2012. Vesiclepedia: a compendium for extracellular vesicles with continuous community annotation. *PLoS Biology*, 10(12), p.e1001450.

Kao, F.F. and Ray, L.H., 1954. Regulation of cardiac output in anesthetized dogs during induced muscular work. *American Journal of Physiology-Legacy Content,* 179(2), pp.255-260.

Kowal, J., Tkach, M. and Théry, C., 2014. Biogenesis and secretion of exosomes. *Current Opinion in Cell Biology*, 29, pp.116-125.

Kowal, J., Arras, G., Colombo, M., Jouve, M., Morath, J.P., Primdal-Bengtson, B., Dingli, F., Loew, D., Tkach, M. and Théry, C., 2016. Proteomic comparison defines novel markers to characterize heterogeneous populations of extracellular vesicle subtypes. *Proceedings of the National Academy of Sciences*, 113(8), pp.E968-E977.

Kugeratski, F.G., Hodge, K., Lilla, S., McAndrews, K.M., Zhou, X., Hwang, R.F., Zanivan, S. and Kalluri, R., 2021. Quantitative proteomics identifies the core proteome of exosomes with syntenin-1 as the highest abundant protein and a putative universal biomarker. *Nature Cell Biology,* 23(6), pp.631-641.

Lancaster, G.I., Møller, K., Nielsen, B., Secher, N.H., Febbraio, M.A. and Nybo, L., 2004. Exercise induces the release of heat shock protein 72 from the human brain in vivo. *Cell Stress & Chaperones,* 9(3), p.276.

Larios, J., Mercier, V., Roux, A. and Gruenberg, J., 2020. ALIX-and ESCRT-III–dependent sorting of tetraspanins to exosomes. *Journal of Cell Biology*, 219(3).

Lee, W.J., Kim, M., Park, H.S., Kim, H.S., Jeon, M.J., Oh, K.S., Koh, E.H., Won, J.C., Kim, M.S., Oh, G.T., Yoon, M., Lee K. and Park J., 2006. AMPK activation increases fatty acid oxidation in skeletal muscle by activating PPARα and PGC-1. *Biochemical and Biophysical Research Communications,* 340(1), pp.291-295.

Liang, B., Peng, P., Chen, S., Li, L., Zhang, M., Cao, D., Yang, J., Li, H., Gui, T., Li, X. and Shen, K., 2013. Characterization and proteomic analysis of ovarian cancer-derived exosomes. *Journal of Proteomics,* 80, pp.171-182.

Linares, R., Tan, S., Gounou, C., Arraud, N. and Brisson, A.R., 2015. High-speed centrifugation induces aggregation of extracellular vesicles. *Journal of Extracellular Vesicles*, 4(1), p.29509.

Maas, S.L., Breakefield, X.O. and Weaver, A.M., 2017. Extracellular vesicles: unique intercellular delivery vehicles. *Trends in Cell Biology,* 27(3), pp.172-188.

Macheda, M.L., Rogers, S. and Best, J.D., 2005. Molecular and cellular regulation of glucose transporter (GLUT) proteins in cancer. *Journal of Cellular Physiology,* 202(3), pp.654-662.

Marsin, A.S., Bouzin, C., Bertrand, L. and Hue, L., 2002. The stimulation of glycolysis by hypoxia in activated monocytes is mediated by AMP-activated protein kinase and inducible 6-phosphofructo-2-kinase. *Journal of Biological Chemistry,* 277(34), pp.30778-30783.

Mentkowski, K.I. and Lang, J.K., 2019. Exosomes engineered to express a cardiomyocyte binding peptide demonstrate improved cardiac retention in vivo. *Scientific Reports,* 9(1), pp.1-13.

Montecalvo, A., Larregina, A.T., Shufesky, W.J., Beer Stolz, D., Sullivan, M.L., Karlsson, J.M., Baty, C.J., Gibson, G.A., Erdos, G., Wang, Z., Milosevic, J., Tkacheva O.A., Divito S.J., Jordan R., Lyons-Weiler J., Watkins S.C., and Morelli A.E., 2012. Mechanism of transfer of functional microRNAs between mouse dendritic cells via exosomes. *Blood, The Journal of the American Society of Hematology*, 119(3), pp.756-766.

Moon, H.Y., Becke, A., Berron, D., Becker, B., Sah, N., Benoni, G., Janke, E., Lubejko, S.T., Greig, N.H., Mattison, J.A., Duzel, E. and van Praag H., 2016. Running-induced systemic cathepsin B secretion is associated with memory function. *Cell Metabolism,* 24(2), pp.332-340.

Mulcahy, L.A., Pink, R.C. and Carter, D.R.F., 2014. Routes and mechanisms of extracellular vesicle uptake. *Journal of Extracellular Vesicles,* 3(1), p.24641.

Ostrowski, M., Carmo, N.B., Krumeich, S., Fanget, I., Raposo, G., Savina, A., Moita, C.F., Schauer, K., Hume, A.N., Freitas, R.P., Goud, B., Benaroch P., Hacohen N., Fukuda M., Desnos C., Seabra M.C., Darchen F., Amigorena S., Moita L.F., and Théry C. 2010. Rab27a and Rab27b control different steps of the exosome secretion pathway. *Nature Cell Biology*, 12(1), pp.19-30.

Pan, B.T., Teng, K., Wu, C., Adam, M. and Johnstone, R.M., 1985. Electron microscopic evidence for externalization of the transferrin receptor in vesicular form in sheep reticulocytes. *The Journal of Cell Biology*, 101(3), pp.942-948.

Park, J., Rho, H.K., Kim, K.H., Choe, S.S., Lee, Y.S. and Kim, J.B., 2005. Overexpression of glucose-6-phosphate dehydrogenase is associated with lipid dysregulation and insulin resistance in obesity. *Molecular and Cellular Biology,* 25(12), pp.5146-5157.

Patel, M.S. and Korotchkina, L.G., 2006. Regulation of the pyruvate dehydrogenase complex. *Biochemical Society Transactions,* 34(2), pp.217-222.

Pedersen, B.K., Steensberg, A., Fischer, C., Keller, C., Keller, P., Plomgaard, P., Febbraio, M. and Saltin, B., 2003. Searching for the exercise factor: is IL-6 a candidate?. *Journal of Muscle Research & Cell Motility*, 24(2-3), p.113.

Pegtel, D.M. and Gould, S.J., 2019. Exosomes. *Annual Review of Biochemistry,* 88, pp.487-514.

Rao, R.R., Long, J.Z., White, J.P., Svensson, K.J., Lou, J., Lokurkar, I., Jedrychowski, M.P., Ruas, J.L., Wrann, C.D., Lo, J.C., Camera, D.M., Lachey J., Gygi S., Seehra J., Hawley J.A., and Spiegelman B.M., 2014. Meteorin-like is a hormone that regulates immune-adipose interactions to increase beige fat thermogenesis. *Cell,* 157(6), pp.1279-1291.

Raposo, G. and Stoorvogel, W., 2013. Extracellular vesicles: exosomes, microvesicles, and friends. *Journal of Cell Biology*, 200(4), pp.373-383.

Reibe, S., Hjorth, M., Febbraio, M.A. and Whitham, M., 2018. GeneXX: an online tool for the exploration of transcript changes in skeletal muscle associated with exercise. *Physiological Genomics,* 50(5), pp.376-384.

Rossetti, L. and Giaccari A., 1990. Relative contribution of glycogen synthesis and glycolysis to insulin-mediated glucose uptake. A dose-response euglycemic clamp study in normal and diabetic rats. *Journal of Clinical Investigation*, 85 (1990), pp. 1785-1792.

Safdar, A., Saleem, A. and Tarnopolsky, M.A., 2016. The potential of endurance exercise-derived exosomes to treat metabolic diseases. *Nature Reviews Endocrinology,* 12(9), p.504.

Sahlin, K., Tonkonogi, M. and Söderlund, K., 1998. Energy supply and muscle fatigue in humans. *Acta Physiologica Scandinavica,* 162(3), pp.261-266.

Sano, S., Izumi, Y., Yamaguchi, T., Yamazaki, T., Tanaka, M., Shiota, M., Osada-Oka, M., Nakamura, Y., Wei, M., Wanibuchi, H., Iwao, H. and Yoshiyama M., 2014. Lipid synthesis is promoted by hypoxic adipocyte-derived exosomes in 3T3-L1 cells. *Biochemical and Biophysical Research Communications*, 445(2), pp.327-333.

Savina, A., Fader, C.M., Damiani, M.T. and Colombo, M.I., 2005. Rab11 promotes docking and fusion of multivesicular bodies in a calcium-dependent manner. *Traffic*, 6(2), pp.131-143.

Shackelford, D.B. and Shaw, R.J., 2009. The LKB1–AMPK pathway: metabolism and growth control in tumour suppression. *Nature Reviews Cancer,* 9(8), pp.563-575.

Sinha, A., Ignatchenko, V., Ignatchenko, A., Mejia-Guerrero, S. and Kislinger, T., 2014. In-depth proteomic analyses of ovarian cancer cell line exosomes reveals differential enrichment of functional categories compared to the NCI 60 proteome. *Biochemical and Biophysical Research Communications,* 445(4), pp.694-701.

Stoppani, J., Hildebrandt, A.L., Sakamoto, K., Cameron-Smith, D., Goodyear, L.J. and Neufer, P.D., 2002. AMP-activated protein kinase activates transcription of the UCP3 and HKII genes in rat skeletal muscle. *American Journal of Physiology-Endocrinology and Metabolism,* 283(6), pp.E1239-E1248.

Taylor, E.B., An, D., Kramer, H.F., Yu, H., Fujii, N.L., Roeckl, K.S., Bowles, N., Hirshman, M.F., Xie, J., Feener, E.P. and Goodyear, L.J., 2008. Discovery of TBC1D1 as an insulin-, AICAR-, and contraction-stimulated signalling nexus in mouse skeletal muscle. *Journal of Biological Chemistry,* 283(15), pp.9787-9796.

Théry, C., Boussac, M., Véron, P., Ricciardi-Castagnoli, P., Raposo, G., Garin, J. and Amigorena, S., 2001. Proteomic analysis of dendritic cell-derived exosomes: a secreted subcellular compartment distinct from apoptotic vesicles. *The Journal of Immunology*, 166(12), pp.7309-7318.

Théry, C., Witwer, K.W., Aikawa, E., Alcaraz, M.J., Anderson, J.D., Andriantsitohaina, R., Antoniou, A., Arab, T., Archer, F., Atkin-Smith, G.K., Ayre, D.C., … Zuba-Surma W.K., et al, 2018. Minimal information for studies of extracellular vesicles 2018 (MISEV2018): a position statement of the International Society for Extracellular Vesicles and update of the MISEV2014 guidelines. *Journal of Extracellular Vesicles,* 7(1), p.1535750.

Tian, T., Zhu, Y.L., Hu, F.H., Wang, Y.Y., Huang, N.P. and Xiao, Z.D., 2013. Dynamics of exosome internalization and trafficking. *Journal of Cellular Physiology*, 228(7), pp.1487-1495.

Tian, Y., Li, S., Song, J., Ji, T., Zhu, M., Anderson, G.J., Wei, J. and Nie, G., 2014. A doxorubicin delivery platform using engineered natural membrane vesicle exosomes for targeted tumor therapy. *Biomaterials,* 35(7), pp.2383-2390.

Tkach, M. and Théry, C., 2016. Communication by extracellular vesicles: where we are and where we need to go. *Cell*, 164(6), pp.1226-1232.

Vader, P., Mol, E.A., Pasterkamp, G. and Schiffelers, R.M., 2016. Extracellular vesicles for drug delivery. *Advanced Drug Delivery Reviews,* 106, pp.148-156.

Valadi, H., Ekström, K., Bossios, A., Sjöstrand, M., Lee, J.J. and Lötvall, J.O., 2007. Exosome-mediated transfer of mRNAs and microRNAs is a novel mechanism of genetic exchange between cells. *Nature Cell Biology*, 9(6), pp.654-659.

Vanderboom, P.M., Dasari, S., Ruegsegger, G.N., Pataky, M.W., Lucien, F., Heppelmann, C.J., Lanza, I.R. and Nair, K.S., 2021. A size-exclusion-based approach for purifying extracellular vesicles from human plasma. *Cell Reports Methods,* 1(3), p.100055.

Van Deun, J., Mestdagh, P., Agostinis, P., Akay, Ö., Anand, S., Anckaert, J., Martinez, Z.A., Baetens, T., Beghein, E., Bertier, L., Berx, G., … Hendrix A., et al, 2017 EV-TRACK: transparent reporting and centralizing knowledge in extracellular vesicle research. *Nature Methods,* 14(3), pp.228-232.

Whitham, M., Parker, B.L., Friedrichsen, M., Hingst, J.R., Hjorth, M., Hughes, W.E., Egan, C.L., Cron, L., Watt, K.I., Kuchel, R.P., Jayasooriah, N., Estevez E., Petzold T., Suter C.M., Gregorevic P., Kiens B., Richter E.A., James D.E., Wojtaszewski J.F.P. and Febbraio M.A., 2018. Extracellular vesicles provide a means for tissue crosstalk during exercise. *Cell Metabolism*, 27(1), pp.237-251.

Wu, N., Zheng, B., Shaywitz, A., Dagon, Y., Tower, C., Bellinger, G., Shen, C.H., Wen, J., Asara, J., McGraw, T.E., Kahn, B.B. and Cantley L.C., 2013. AMPK-dependent degradation of TXNIP upon energy stress leads to enhanced glucose uptake via GLUT1. *Molecular Cell,* 49(6), pp.1167-1175.

Zhao, H., Yang, L., Baddour, J., Achreja, A., Bernard, V., Moss, T., Marini, J.C., Tudawe, T., Seviour, E.G., San Lucas, F.A., Alvarez, H., Gupta S., Maiti S.N., Cooper L., Peehl

D., Ram P.T., Maitra A. and Nagrath D., 2016. Tumor microenvironment derived exosomes pleiotropically modulate cancer cell metabolism. *Elife*, 5, p.e10250.